The contribution of an electric dipole–dipole mechanism can be expressed as[23]

$$k_{DA}^{dd} = \frac{1}{\epsilon^2}\left(\frac{3c}{8\pi^2}\right)\frac{e^4}{m^2c^4}\left(\frac{f_D f_A}{\tilde{\nu}_{DA}^2 R_{DA}^6}\right)\Omega_{DA} \qquad (7)$$

where f_D and f_A are the donor and acceptor oscillator strengths, respectively, R_{DA} is the donor–acceptor distance, and $\tilde{\nu}_{DA}$ is the energy of the region of overlap. The remaining symbols in eq 7 have their usual meaning. In our situation, we obtain, from the absorption spectrum, $f_D \approx 6 \times 10^{-6}$ and $f_A \approx 2 \times 10^{-5}$. The shortest meaningful contact, which is the distance between ligand centers on neighboring complexes in the crystal, is 4.995 Å.[11] We obtain, in the dipole approximation, $k_{hh} \approx 5 \times 10^6$ s^{-1}. The electric dipole–dipole mechanism thus makes a minor contribution to the total transfer rate. The dominant part originates from exchange or higher multipole interactions. In organic molecular crystals, rate constants for transfer between host molecules of the order of $k_{hh} = 10^{11}$ s^{-1} have been reported, and also in these systems the contribution from a dipole–dipole mechanism was found to be negligible.[24]

Conclusions

High-resolution laser spectroscopy at cryogenic temperatures provides a very detailed picture of the complexes $[Rh(phpy)_2(bpy)]^+$ and $[Rh(thpy)_2(bpy)]^+$. In contrast to the case of conventional low-resolution absorption and luminescence spectroscopy of solutions and glassy matrices, we clearly identify two excited states separated by 22 and 156 cm^{-1} in [PhpyBpy]PF_6 and [ThpyBpy]-doped [PhpyBpy]PF_6, respectively. Their energy separation strongly depends on the environment for a given complex. In contrast, the vibrational energy pattern, which can be determined very accurately, is essentially independent of the environment. By doping [ThpyBpy] into [PhpyBpy]PF_6, we have achieved two major goals. Due to the sharpness of the luminescence and excitation spectra, we obtain an accurate picture of the ground- and excited-state properties of the [ThpyBpy] complex. The luminescent excitation traps in [PhpyBpy]PF_6 are identified, and they allow us to elucidate the excitation-transfer processes in the host lattice.

Acknowledgment. This work was financially supported by the Swiss National Science Foundation. We acknowledge a loan of $RhCl_3$ from Degussa.

Registry No. $[Rh(phpy)_2(bpy)]PF_6$, 108456-27-5; $[Rh(thpy)_2(bpy)]PF_6$, 127064-80-6.

(23) Di Bartolo, B. *Optical Interactions in Solids*; Wiley: New York, 1968; Chapter 18.4.
(24) Güttler, W.; von Schütz, J. U.; Wolf, H. C. *Chem. Phys.* **1977**, *24*, 159.
(25) Colombo, M. G. Unpublished results.
(26) Weinzierl, G.; Friedrich, J. *Chem. Phys. Lett.* **1981**, *83*, 204.
(27) Shelby, R. M.; Zewail, A. H.; Harris, C. B. *J. Chem. Phys.* **1976**, *64*, 3192.

Contribution from the Laboratoire de Photochimie, Electrochimie et Chimie Moléculaire, Unité Associée au CNRS D0322, Université de Bretagne Occidentale, 29287 Brest Cedex, France, and Department of Chemistry, Stanford University, Stanford, California 94305

Electrochemical and Spectroscopic Properties of Dimeric Cofacial Porphyrins with Nonelectroactive Metal Centers. Delocalization Processes in the Porphyrin π-Cation-Radical Systems

Yves Le Mest,*[1a] Maurice L'Her,*[1a] Neil H. Hendricks,[1b] Kimoon Kim,[1b] and James P. Collman[1b]

Received July 24, 1991

The proximity of two or more porphyrins has been shown to be crucial in numerous biological processes such as electron transfer or oxygen activation. We report the electrochemical and spectroscopic (UV–vis, EPR) behavior of two families of dimeric cofacial diporphyrins, either covalently linked by two amide bridges (FTF*n* family) or monolinked by a polyaromatic bridge ("Pacman" DPX family). The derivatives with nonelectroactive centers (H_2, Zn, Cu) are investigated; thus the redox systems are centered on the π-ring systems only. When the two rings are sufficiently far apart, the dimer nearly behaves as the juxtaposition of two monomers. A two-electron oxidation process formally gives rise to a π-cation diradical, and in one case a triplet-state spectrum can be observed. When the two rings are very close, strong π–π interactions generate mixed-valence behavior: the first oxidation process is split into two one-electron steps. The first oxidation product is a totally delocalized π-radical, while in the second the two delocalized electrons of the rings become spin-paired, giving rise to a kind of nonclassical π–π bond. Analysis of the results and rationalization with the literature demonstrate that from a redox standpoint these molecules have to be considered as a single redox entity. A qualitative molecular orbital diagram is proposed which accounts for the enhanced electronic properties of these dimers.

Introduction

Recent growing interest in the chemistry of polynuclear porphyrin and phthalocyanine derivatives, either natural or synthetic aggregates, sandwich complexes, or covalently linked oligomers, derives from their remarkable electron-transfer properties. Porphyrins have been shown to be interesting models of photosystems for energy conversion[2-11] as well as to display molecular conductivity.[11] Another area in which closely spaced porphyrinic systems are known to be involved is catalysis in natural systems

(1) (a) Université de Bretagne Occidentale. (b) Stanford University.
(2) Deisenhofer, J.; Epp, O.; Miki, K.; Huber, R.; Michel, H. *J. Mol. Biol.* **1984**, *180*, 385.
(3) Chang, C. H.; Tiede, D.; Tang, J.; Smith, U.; Norris, J.; Schiffer, M. *FEBS Lett.* **1986**, *205*, 82.
(4) Wasielewski, M. R. In *Photoinduced Electron Transfer*; Fox, M. A., Chanon, M., Eds.; Elsevier: Amsterdam, 1988; p 161.
(5) (a) Warshel, A. *Proc. Natl. Acad. Sci. U.S.A.* **1980**, *77*, 3105. (b) Warshel, W.; Parson, W. W. *J. Am. Chem. Soc.* **1987**, *109*, 6143. (c) Parson, W. W.; Warshel, A. *J. Am. Chem. Soc.* **1987**, *109*, 6152.
(6) Boxer, S. G. *Biochim. Biophys. Acta* **1983**, *726*, 265.
(7) McLendon, G. *Acc. Chem. Res.* **1988**, *21*, 160.
(8) Volkov, A. G. *J. Electroanal. Chem. Interfacial Electrochem.* **1986**, *205*, 245.
(9) (a) Thompson, M. A.; Zerner, M. C.; Fajer, J. *J. Phys. Chem.* **1990**, *94*, 3820. (b) Smith, K. M.; Kehres, L. A.; Fajer, J. *J. Am. Chem. Soc.* **1983**, *105*, 1387.

0020-1669/92/1331-0835$03.00/0

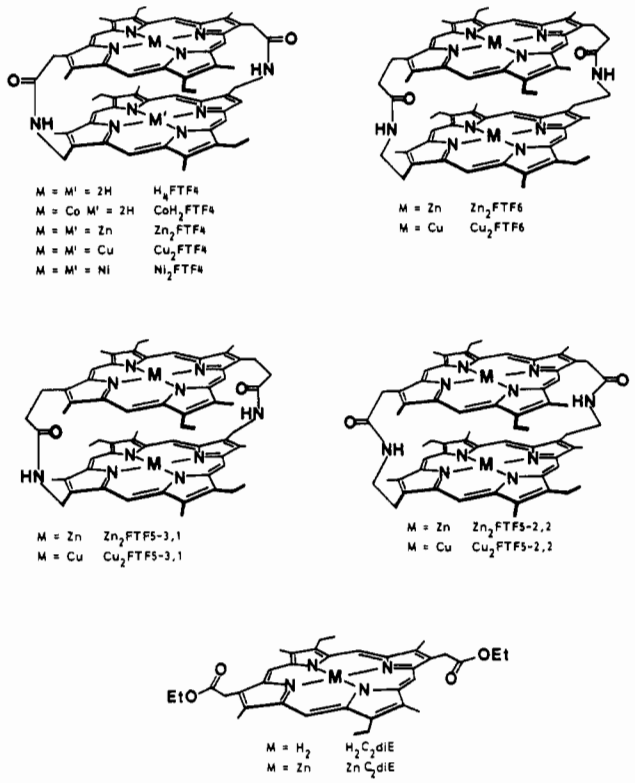

Figure 1. Porphyrins investigated in the present study: FTF*n* series.[13a,i]

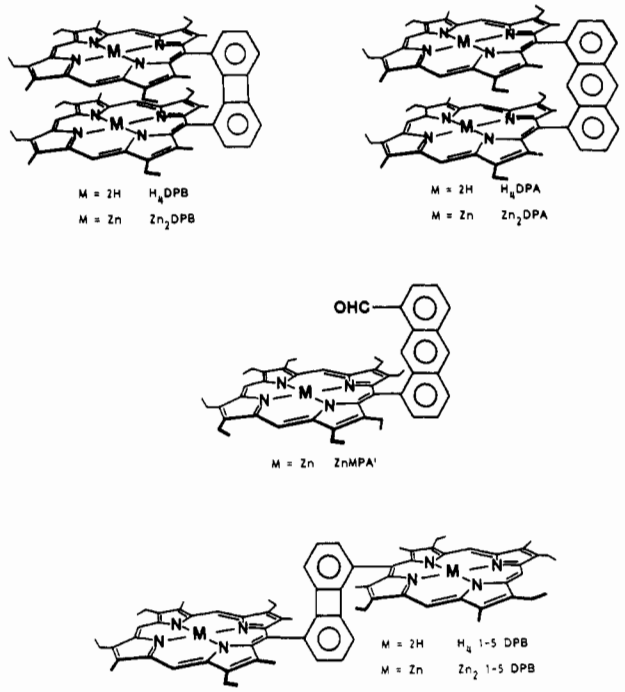

Figure 2. Porphyrins investigated in the present study: "Pacman" DP series.[26]

Scheme I. General Redox Pathway for the Oxidation or Reduction of a Porphyrin Ring[a]

$$[MP] \underset{E_{ox}(1)}{\overset{-e}{\rightleftharpoons}} [MP^{\bullet}]^{+} \underset{E_{ox}(2)}{\overset{-e}{\rightleftharpoons}} [MP]^{2+} \quad (1)$$

$$[MP] \underset{E_{red}(1)}{\overset{+e}{\rightleftharpoons}} [MP^{\bullet}]^{-} \underset{E_{red}(2)}{\overset{+e}{\rightleftharpoons}} [MP]^{2-} \quad (2)$$

[a] P = porphyrin ring; M = nonelectroactive metal.

(hemoglobin, cytochromes, ...) and particularly in oxygen activation.[12] In a synthetic approach, this was especially emphasized by the discovery of Collman[13] and sometime afterward by Chang[14] of face-to-face diporphyrins capable of reducing dioxygen to water by a four-electron mechanism. The originally studied natural or synthetic aggregates of molecules are now giving way to covalently linked oligomers,[13-16,19] or sandwich systems,[17,18] which allow a much better control of structure during redox and/or chemical processes. Even though it is clearly evident that strong $\pi-\pi$

(10) (a) Netzel, T. L.; Kroger, P.; Chang, C. K.; Fujita, I.; Fajer, J. *Chem. Phys. Lett.* **1979**, *67*, 223. (b) Netzel, T. L.; Bergkamp, M. A.; Chang, C. K. *J. Am. Chem. Soc.* **1982**, *104*, 1952.

(11) Hoffman, B.; Ibers, J. A. *Acc. Chem. Res.* **1983**, *16*, 15.

(12) (a) *Metal Ion Activation of Dioxygen*; Spiro, T. G., Ed.; Wiley: New York, 1980. (b) *The Porphyrins*; Dolphin, D., Ed.; Academic Press: New York, 1978. (c) Chang, C. K.; Wang, C. B. Binuclear Porphyrin Complexes. In *Electron Transport and Oxygen Utilization*; Chien, H., Ed.; Elsevier: Amsterdam, 1982; p 237. (d) Collman, J. P.; Anson, F. C.; Bencosme, S.; Chong, A.; Collins, T.; Denisevich, P.; Evitt, E.; Geiger, T.; Ibers, J.; Jameson, G.; Konai, Y.; Koval, C.; Meier, K.; Oakley, R.; Pettman, R.; Schmittou, E.; Sessler, J. In *Organic Synthesis Today and Tomorrow*; Trost, B. M., Hutchinson, C. R., Eds.; Pergamon Press: New York, 1981; p 29.

(13) (a) Collman, J. P.; Marrocco, M.; Denisevich, P.; Koval, C.; Anson, F. C. *J. Electroanal. Chem. Interfacial Electrochem.* **1979**, *101*, 117. (b) Collman, J. P.; Denisevich, P.; Konai, Y.; Marrocco, M.; Koval, C.; Anson, F. C. *J. Am. Chem. Soc.* **1980**, *102*, 6027. (c) Durand, R. R.; Bencosme, C. S.; Collman, J. P.; Anson, F. C. *J. Am. Chem. Soc.* **1983**, *105*, 2710. (d) Collman, J. P.; Bencosme, C. S.; Barnes, C. E.; Miller, B. D. *J. Am. Chem. Soc.* **1983**, *105*, 2704. (e) Collman, J. P.; Anson, F. C.; Barnes, C. E.; Bencosme, C. S.; Geiger, T.; Evitt, E. R.; Kreh, R. P.; Meier, K.; Pettman, R. P. *J. Am. Chem. Soc.* **1983**, *105*, 2694. (f) Collman, J. P.; Bencosme, C. S.; Durand, R. R.; Kreh, R. P.; Anson, F. C. *J. Am. Chem. Soc.* **1983**, *105*, 2699. (g) Durand, R. R.; Collman, J. P.; Anson, F. C. *J. Electroanal. Chem. Interfacial Electrochem.* **1983**, *151*, 289. (h) Collman, J. P.; Hendricks, N. H.; Kim, K.; Bencosme, C. S. *J. Chem. Soc., Chem. Commun.* **1987**, 1537. (i) Ngameni, E.; Le Mest, Y.; L'Her, M.; Collman, J. P.; Hendricks, N. H.; Kim, K. *J. Electroanal. Chem. Interfacial Electrochem.* **1987**, *220*, 247. (j) Collman, J. P.; Hendricks, N. H.; Leidner, C. R.; Ngameni, E.; L'Her, M. *Inorg. Chem.* **1988**, *27*, 387.

(14) (a) Liu, H. Y.; Weaver, M. J.; Wang, C. B.; Chang, C. K. *J. Electroanal. Chem. Interfacial Electrochem.* **1983**, *145*, 439. (b) Chang, C. K.; Liu, H. Y.; Abdalmuhdi, I. *J. Am. Chem. Soc.* **1984**, *106*, 2725. (c) Ni, C.-L.; Abdalmuhdi, I.; Chang, C. K.; Anson, F. C. *J. Phys. Chem.* **1987**, *91*, 1158. (d) Liu, H.-Y.; Abdalmuhdi, I.; Chang, C. K.; Anson, F. C. *J. Phys. Chem.* **1985**, *89*, 665.

(15) (a) Cowan, J. A.; Sanders, J. K. M. *J. Chem. Soc., Chem. Commun.* **1985**, 1213. (b) *J. Chem. Soc., Chem. Commun.* **1985**, 1214. (c) Cowan, J. A.; Sanders, J. K. M.; Beddard, G. S.; Harrison, R. J. *J. Chem. Soc., Chem. Commun.* **1987**, 55. (d) Leighton, P.; Sanders, J. K. M. *J. Chem. Soc., Perkin Trans. 1* **1987**, 2385. (e) Cowan, J. A.; Sanders, J. K. M. *J. Chem. Soc., Perkin Trans. 1* **1987**, 2395. (f) Leighton, P.; Cowan, J. A.; Abraham, R. J.; Sanders, J. K. M. *J. Org. Chem.* **1988**, *53*, 733. (g) Hunter, C. A.; Sanders, J. K. M.; Stone, A. J. *Chem. Phys.* **1989**, *133*, 395. (h) Naylor, S.; Hunter, C. A.; Cowan, J. A.; Lamb, J. H.; Sanders, J. K. M. *J. Am. Chem. Soc.* **1990**, *112*, 6507. (i) Cowan, J. A. *J. Chem. Soc., Dalton Trans.* **1988**, 2681. (j) Hunter, C. A.; Leighton, P.; Sanders, J. K. M. *J. Chem. Soc., Perkin Trans. 1* **1989**, 547. (k) Hunter, C. A.; Sanders, J. K. M. *J. Am. Chem. Soc.* **1990**, *112*, 5525.

(16) (a) Nevin, W. A.; Hempstead, M. R.; Liu, W.; Leznoff, C. C.; Lever, A. B. P. *Inorg. Chem.* **1987**, *26*, 570. (b) Nevin, W. A.; Liu, W.; Greenberg, S.; Hempstead, M. R.; Marcuccio, S. M.; Melnik, M.; Leznoff, C. C.; Lever, A. B. P. *Inorg. Chem.* **1987**, *26*, 891. (c) Leznoff, C. C.; Lam, H.; Nevin, W. A.; Kobayashi, N.; Janda, P.; Lever, A. B. P. *Angew. Chem., Int. Ed. Engl.* **1987**, *26*, 1021. (d) Manivannan, V.; Nevin, W. A.; Leznoff, C. C.; Lever, A. B. P. *Coord. Chem.* **1988**, *19*, 139. (e) Kobayashi, N.; Lam, H.; Nevin, W. A.; Janda, P.; Leznoff, C. C.; Lever, A. B. P. *Inorg. Chem.* **1990**, *29*, 3415.

(17) (a) DeWulf, D. W.; Leland, J. K.; Wheeler, B. L.; Bard, A. J.; Batzel, D. A.; Dininny, D. R.; Kenney, M. E. *Inorg. Chem.* **1987**, *26*, 266. (b) Simic-Glavaski, B.; Tanaka, A. A.; Kenney, M. E.; Yeager, E. *J. Electroanal. Chem. Interfacial Electrochem.* **1987**, *229*, 285. (c) Anderson, A. B.; Gordon, T. L.; Kenney, M. E. *J. Am. Chem. Soc.* **1985**, *107*, 192. (d) Wheeler, B. L.; Nagasubramanian, G.; Bard, A. J.; Schechtman, L. A.; Dininny, D. R.; Kenney, M. E. *J. Am. Chem. Soc.* **1984**, *106*, 7404. (e) Mezza, T. M.; Armstrong, N. R.; Ritter, G. W., II; Iafalice, J. P.; Kenney, M. E. *J. Electroanal. Chem. Interfacial Electrochem.* **1982**, *137*, 227.

(18) (a) Donohoe, R. J.; Duchowski, J. K.; Bocian, D. F. *J. Am. Chem. Soc.* **1988**, *110*, 6119. (b) Duchowski, J. K.; Bocian, D. F. *Inorg. Chem.* **1990**, *29*, 4158. (c) Duchowski, J. K.; Bocian, D. F. *J. Am. Chem. Soc.* **1990**, *112*, 3312.

interactions exist between the two rings of the molecule, the role of this kind of interaction has not been shown to be involved in catalytic processes. Thus far, the bimetallic nature of the dimers, with the possible intervention of metal–metal interactions, has been proposed to be the origin of the improved catalytic efficiency.[13,14,20] In the present paper, we intend to demonstrate that the coupling of these systems in a cofacial configuration induces a so-called "cofacial effect" which is both electronic and steric. This effect originates in strong interactions between the two π-ring systems, inducing a great enhancement of the electron density in the neutral form of these dimers, whereas electron delocalization over the two rings is observed in the case of their oxidized forms. The discussion of the present results and rationalization with the literature on closely spaced porphyrinic systems allow one to propose a model for the interactions of this type of face-to-face dimers, which demonstrates that these dimers have to be considered as a single redox entity, as opposed to two juxtaposed monomers. This model accounts for the peculiar enhanced electronic properties of the π systems, but as well affords new insight into the improved catalytic behavior toward dioxygen reduction of the dicobalt derivatives.

Our interest in cofacial diporphyrins was initiated as a study of the special properties of the dicobalt derivatives which could explain their efficiency in the catalytic four-electron reduction mechanism of O_2.[21,22] Our previous studies, limited to cobalt derivatives, allowed us to demonstrate that these possess peculiar properties and reactivity toward dioxygen as compared to monomers. Particularly striking was the observation of mixed-valence derivatives[21] with an unprecedented reactivity toward dioxygen.[22] However, it quickly developed that this unique reactivity toward dioxygen could not be understood, as previously postulated, on the only basis of a bimetallic concept, even taking into account evident metal–metal interactions. Owing to strong perturbations due to the dimeric nature of the ligand, the assignment of the redox processes, either cobalt or ring centered, is difficult to ascertain.[21] In order to understand the situation, it became necessary to examine the properties of the ligand itself; thus derivatives of these dimers were studied as the free bases or as complexes with nonelectroactive metals. This is the topic of this paper. A forthcoming paper[21c,d] will deal with the admixture of the redox exchanges centered on the metal in the case of cobalt with those on the rings. The compounds investigated, in the present paper, are depicted in Figures 1 and 2. For these, the electrochemical reactions take place only on the π ring of the porphyrins, never on the metal as is the case for cobalt derivatives (Co^{III}/Co^{II} and Co^{II}/Co^{I}).

The electrochemical behavior of porphyrins complexed by stable divalent nonelectroactive metals (such as Zn^{2+}, Mg^{2+}, Cu^{2+}, ...) or of the free base (H_2P) is very well-known.[24,25] The oxidation (or reduction) of the π ring proceeds through two reversible one-electron processes (as shown in Scheme I), leading, in the first reaction, to the formation of a π-cation (or π-anion) radical in which an electron is delocalized over the porphyrin and, in the second reaction, to a dication (or dianion).

Many studies on the electrochemical behavior of face-to-face porphyrins, either covalently linked oligomers, aggregates, or sandwiches, are emerging,[19] but hitherto none of them has clearly emphasized and systematically rationalized the strong redox interactions of the face-to-face systems. Recently strong π–π interactions of this sort have been demonstrated with phthalocyanines.[16,17] Some of these are covalently linked and are closely related to the DPA and DPB models in Figure 2, complexed with nonelectroactive metals; the dicobalt derivatives behave similarly to our porphyrin derivatives.[17] Redox interactions have been detected and analyzed in face-to-face stacked-ring silicon phthalocyanines as well.[17] However, these results do not allow much extrapolation to our diporphyrinic systems, since it is well-known that the mutual energy levels of the rings and cobalt are different in both cases. Would that account for the inefficacy of the cobalt derivatives of the DPA and DPB phthalocyanines[16e] compared with the porphyrin analogues which are efficient catalysts[14b-d] for the reduction of O_2?

The electrochemical investigations were performed in aprotic solutions, mainly benzonitrile (PhCN). The neutral and first-process oxidized (abstraction of one equivalent-electron per ring) derivatives were characterized by UV–visible spectrophotometry and EPR spectroscopy. In the following we will designate by first (or second) oxidation *process* the reaction leading to the virtual formation of the π-cation, one electron per ring (or dication, a second electron abstracted per each ring), and the same for the reduction. For clarity, a discrimination, between *process* and *step*, in the case of these dimers needs to be pointed out insofar as each redox *process* can take place either in one two-electron *step* or in two one-electron redox *steps*.

Experimental Section

As the compounds used in the present work are obtained at very low yields after long synthetic routes, the available quantities for electrochemistry were very low (a few milligrams for each). This means that each experiment had to be performed on a very small fraction (0.2–0.3 mg) dissolved in minute volumes (ca. 300 μL). Furthermore, the solubility of these compounds is low (0.7–0.5 mM). For these reasons, some of the quantitative measurements were obtained with a limited precision.

Owing to the extreme sensitivity of these dimers to traces of oxygen and water, all experiments were carried out in a dry nitrogen atmosphere box with carefully deoxygenated solvents and chemicals.

Chemicals. The synthesis, purification, and characterization of the diporphyrins of the FTF*n* series[13] and the DPX (X = A or B) "Pacman" series[26] have been described in detail elsewhere. They were all synthesized at Stanford.

(19) (a) Becker, J. Y.; Dolphin, D.; Paine, J. B.; Wijesekera, T. *J. Electroanal. Chem. Interfacial Electrochem.* **1984**, *164*, 335. (b) Williams, R. F. X.; White, D.; Hambright, P.; Shanim, A.; Little, R. G. *Bioelectrochem. Bioenerg.* **1983**, *10*, 69. (c) Lexa, D.; Maillard, P.; Momenteau, M.; Savéant, J. M. *J. Am. Chem. Soc.* **1984**, *106*, 6321. (d) Buchler, J. W.; Elsässer, K.; Kihn-Botulinski, M.; Scharbert, B. *Angew. Chem., Int. Ed. Engl.* **1986**, *25*, 286. (e) Osuka, A.; Maruyama, K. *Chem. Lett.* **1987**, 825. (f) Collman, J. P.; Marrocco, M.; Elliott, C. M.; L'Her, M. *J. Electroanal. Chem. Interfacial Electrochem.* **1981**, *124*, 113. (g) Kadish, K. M.; Larson, G.; Lexa, D.; Momenteau, M. *J. Am. Chem. Soc.* **1975**, *97*, 282. (h) Wasielewski, M. R.; Svec, W. A.; Cope, B. T. *J. Am. Chem. Soc.* **1978**, *100*, 1961. (i) Sessler, J. L.; Johnson, M. R.; Lin, T. Y.; Creager, S. E. *J. Am. Chem. Soc.* **1988**, *110*, 3659.

(20) (a) Yeager, E. *J. Electrochem. Soc.* **1981**, *128*, 160C. (b) Yeager, E. *Electrochim. Acta* **1984**, *29*, 1527. (c) Elzing, A.; van der Putten, A.; Visscher, W.; Barendrecht, E. *Recl. Trav. Chim. Pays-Bas* **1990**, *109*, 31. (d) van der Putten, A.; Elzing, A.; Visscher, W.; Barendrecht, E.; Harcourt, R. D. *Theochem* **1988**, *180*, 309. (e) Vasudevan, P.; Santoosh; Mann, N.; Tyagi, S. *Transition Met. Chem. (London)* **1990**, *15*, 81.

(21) (a) Le Mest, Y.; L'Her, M.; Collman, J. P.; Kim, K.; Hendricks, N. H.; Helm, S. *J. Electroanal. Chem. Interfacial Electrochem.* **1987**, *234*, 277. (b) Le Mest, Y.; L'Her, M.; Courtot-Coupez, J.; Collman, J. P.; Evitt, E. R.; Bencosme, C. S. *J. Electroanal. Chem. Interfacial Electrochem.* **1985**, *184*, 331. (c) Le Mest, Y. Thèse d'Etat, Brest, France, 1988. (d) Le Mest, Y.; L'Her, M.; Collman, J. P. To be published.

(22) (a) Le Mest, Y.; L'Her, M.; Collman, J. P.; Hendricks, N. H.; McElwee-White, L. *J. Am. Chem. Soc.* **1986**, *108*, 533. (b) Le Mest, Y.; L'Her, M.; Courtot-Coupez, J.; Collman, J. P.; Evitt, E.; Bencosme, C. S. *J. Chem. Soc., Chem. Commun.* **1983**, 1286.

(23) (a) FTF*n* stands for face-to-face, the Collman series[13] in which the two rings are linked by two amide bridges each constituted of *n* atoms. (b) DPX (X = A or B) stands for diporphyrin anthracene (A) or biphenylene (B), the Chang monolinked "Pacman" dimer series.[14,26]

(24) Recent reviews: (a) Davis, D. G. In ref 12b, Vol. V, p 127. (b) Felton, R. H. In ref 12b, Vol. V, p 53. (c) Kadish, K. M. In *Progress in Inorganic Chemistry*; Lippard, S. J., Ed.; Wiley: New York, 1986; Vol. 34, p 435.

(25) (a) Fuhrhop, J. H.; Kadish, K. M.; Davis, D. G. *J. Am. Chem. Soc.* **1973**, *95*, 5140. (b) Fajer, J.; Borg, D. C.; Forman, A.; Dolphin, D.; Felton, R. H. *J. Am. Chem. Soc.* **1970**, *92*, 3451. (c) Kadish, K. M.; Bottomley, L. A.; Kelly, S.; Schaeper, D.; Shiue, L. R. *Bioelectrochem. Bioenerg.* **1981**, *8*, 213. (d) Wolberg, A.; Manassen, J. *J. Am. Chem. Soc.* **1970**, *92*, 2982. (e) Felton, R. H.; Linschitz, H. *J. Am. Chem. Soc.* **1966**, *88*, 1113. (f) Stanienda, A.; Biebl, G. *Z. Phys. Chem.* **1967**, *52*, 254. (g) Dolphin, D.; Muljiani, Z.; Rousseau, K.; Borg, D. C.; Fajer, J.; Felton, R. H. *Ann. N.Y. Acad. Sci.* **1973**, *203*, 177. (h) Dolphin, D.; Felton, R. H.; Borg, D. C.; Fajer, J. *J. Am. Chem. Soc.* **1970**, *92*, 743.

(26) (a) Chang, C. K.; Abdalmuhdi, I. *Angew. Chem., Int. Ed. Engl.* **1984**, *23*, 164. (b) Chang, C. K.; Abdalmuhdi, I. *J. Org. Chem.* **1983**, *48*, 5388.

Table I. Electrochemical Data for the Zinc, Copper, and Free-Base Mono- and Diporphyrins

porphyrin	ring oxidn: E°/V[a] (ΔE_p/mV),[b] ne[c,d] 1st process	ring oxidn: E°/V[a] (ΔE_p/mV),[b] ne[c,d] 2nd process	ring redn: E°/V[a] (ΔE_p/mV),[b] ne[d] 1st process
		FTF Series	
H_2C2diE	0.39 (60), 1e	0.90 (100), 1e	−1.81 (70), 1e
H_2C3diE	0.34 (70), 1e	0.89 (160), 1e	−1.87 (80), 1e
H_4FTF4	0.16 (70), 1e; 0.39 (70), 1e	1.06 (Irr)[e], 1e	−1.92 (70), 2e
CoH_2FTF4	0.00 (100), 1e; 0.34 (80), 1e	0.80 (Irr),[e] 1e; 1.10 (Irr)[e], 1e	−1.64 (80), 1e; −1.92 (80), 1e
ZnC2diE	0.22 (60), 1e	0.63 (70), 1e	−2.00 (80), 1e
Zn_2FTF6	0.09 (50), 2e	0.65 (70), 2e	−2.05 (60), 1e; −2.20 (80), 1e
Zn_2FTF5 2-2	0.03 (60), 1e; 0.13 (60), 1e	0.76 (140), 2e	−2.05 (60), 1e; −2.18 (70), 1e
Zn_2FTF5 3-1	−0.07 (60), 1e; 0.12 (60), 1e	0.75 (140), 2e	−2.13 (60), 1e; −2.22 (60), 1e
Zn_2FTF4	0.00 (60), 1e; 0.17 (70), 1e	0.75 (90), 2e	−2.06 (50), 2e
Cu_2FTF6	0.18 (140), 2e	0.98 (Irr)[e], 1e	−2.08 (85), 2e
Cu_2FTF5 2-2	0.04 (60), 1e; 0.26 (60), 1e	1.00 (180), 2e	−2.04 (60), 1e; −2.21 (80), 1e
Cu_2FTF5 3-1	−0.05 (60), 1e; 0.26 (60), 1e	0.90 (200), 2e	−2.14 (100), 1e; −2.25 (60), 1e
Cu_2FTF4	0.04 (60), 1e; 0.33 (70), 1e	1.00 (80), 2e	−2.09 (80), 2e
Ni_2FTF4	0.07 (60), 1e; 0.36 (70), 1e	0.98 (160), 2e	−2.08 (100), 2e
		Pacman Series	
H_4DPA	0.31 (60), 1e; 0.43 (60), 1e	0.85 (100), 2e	−1.92 (60), 2e
H_4DPB	0.14 (70), 1e; 0.37 (70), 1e	0.92 (120), 2e; 1.22 (Irr)[e], 1e	−2.06 (120), 2e
ZnMPA′	0.19 (70), 1e	0.52 (70), 1e	−1.95 (60), 1e
$Zn_2$1-5DPB	0.23 (60), 2e	0.54 (100), 2e	−2.05 (70), 2e
Zn_2DPA	0.16 (60), 1e; 0.23 (60), 1e	0.60 (90), 2e	−2.11 (60), 2e
Zn_2DPB	0.06 (70), 1e; 0.21 (70), 1e	0.64 (70), 1e; 0.85 (100), 1e	−2.15 (70), 1e; −

[a] Obtained from cyclic voltammetry in PhCN + Bu_4NPF_6; Pt button; 100 mV/s; E° versus Fc^+/Fc. [b] $\Delta E_p = E_{pa} - E_{pc}$. [c] ne = number of electrons exchanged; measured by coulometry for the first oxidation processes of the zinc compounds with an uncertainty of 5%. [d] n values for the other systems were derived from the comparison of the diffusion currents (on the wave of RDE voltammetry) and/or CV peak heights to those of zinc compounds; uncertainty was less than 20%. [e] Anodic peak potentials.

The solvent (mainly benzonitrile (PhCN)) and the supporting electrolyte, tetrabutylammonium hexafluorophosphate (Bu_4NPF_6) were purified as previously described.[22] Dichloromethane (CH_2Cl_2) from Merck was used in special cases, e.g. electrochemical preparation of the EPR samples; as the results in this solvent were not significantly different and the study was not extended systematically to all the compounds, the results are not listed. Solutions of the supporting electrolyte were prepared in the drybox, stored over molecular sieves (Linde 4 Å), and twice percolated through an activated (400 °C under vacuum for 48 h) neutral alumina (Merck) column.

To record the spectra, solutions were transferred to EPR tubes or to UV–vis cuvettes, sealed before removal from the drybox.

Apparatus. The drybox was manufactured by Jaram; the nitrogen flow was continuously purified by passage through molecular sieves at ambient temperature and divided copper BTS catalyst (BASF) at 100 °C.

The electrochemical cell was especially designed to fit the rotating disk electrode (EDI Tacussel) for a minimum volume of solution in the main compartment. The auxiliary electrode and the reference (ferrocenium/ferrocene (Fc^+/Fc)) were in separated compartments connected to the main one through ground joints terminated by frits (Vycor tips from PAR). For voltammetric measurements, a platinum disk (diameter 2 mm) was employed; the electrolyses were performed with the same electrode equipped with a 4 mm diameter disk. For the purpose of comparison, the formal potential of Fc^+/Fc versus SCE is 0.43 V measured in the same medium (PhCN, 0.2 M Bu_4NPF_6).

A PAR Model 173 potentiostat, equipped with a PAR 179 digital coulometric unit, was monitored by a PAR 175 programmer; the chart recorder was a T-2Y SEFRAM ENERTEC. UV–visible spectra were recorded on a Cary 219 spectrophotometer from Varian. A JEOL FE3X apparatus was used for the EPR spectroscopy; spectra were recorded from solutions (V = 40 μL) at a concentration close to 5×10^{-4} M in quartz tubes; power was 1 mW and frequency close to 9.2 GHz.

Results

Electrochemistry. Typical cyclic voltammograms for the two series of cofacial porphyrins in PhCN, 0.2 M Bu_4NPF_6, are presented in Figure 3; the electrochemical data are gathered in Table I. As discussed above, a porphyrin ring can be oxidized (or reduced) in two one-electron steps described in eqs 1 and 2. For the purpose of comparison, the results obtained for some monomers, C_2diE and MPA, are also given in Table I and a voltammogram of the ZnC_2diE is shown in Figure 3: the two oxidation waves can be seen as well as the first reduction wave; the second one is too close to the solvent breakdown to be completely seen. In the case of all the dimers, this second process is even more negative and cannot be observed; thus only the data for the first reduction process ($E_{red}(1)$) are reported.

In the case of all the FTF dimers, only redox systems ascribable to these three processes are observed in the electrochemical window of the solvent (curves b and c). As for the Pacman series, an extra reversible oxidation system is observed at a potential in the 1.3–1.5 V range, as shown in Figure 3d. This is in the range of the pseudoreversible oxidation potential of the aromatic moieties anthracene and biphenylene.[27] The data for these systems are not reported in Table I. No other significant difference is apparent that could account for the different natures of the linking bridges in the two series.

The number of electrons exchanged for each system were determined, by coulometry for the first oxidation process (Cu and Zn), and were equal to integers (n = 1 or 2 ± 5%), except for the case of Zn_2FTF6, for which a value of n = 1.7 ± 0.1 was measured. This was attributed to the presence of an impurity which could be the one seen by cyclic voltammetry (Figure 3b). For all the other redox processes, the number of electrons was obtained by comparison of the peak (CV) and wave (RDE) heights with those of the first oxidation process of the zinc compounds (uncertainty is less than 20%).

As can be seen in Table I, almost all the redox systems for the first oxidation and the first reduction process have a peak separation $\Delta E_p = E_{pa} - E_{pc}$ close to the theoretical value of 60 mV, while the ratio i_{pa}/i_{pc} is close to unity and i_p/v is constant for any scan rate v ($0.01 < v < 1$ V s^{-1}). This indicates diffusion-controlled reversible processes. In some cases, the first oxidation of Zn_2FTF6 and the first reduction of Zn_2FTF4, where two electrons are exchanged at very close potentials, ΔE_p values less than 60 mV are seen, indicative of "cooperative" interactive redox processes.[28] The second oxidation process generally displays ΔE_p values much greater than 60 mV with i_{pa}/i_{pc} ratios more than unity. This is

(27) Peover, M. E. *Electroanal. Chem.* **1967**, *2*, 1.
(28) (a) Flanagan, J. B.; Margel, S.; Bard, A. J.; Anson, F. C. *J. Am. Chem. Soc.* **1978**, *100*, 4248. (b) Polcyn, D. S.; Shain, I. *Anal. Chem.* **1966**, *38*, 370. (c) Myers, R. L.; Shain, I. *Anal. Chem.* **1969**, *41*, 980.
(29) (a) Chang, C. K. *Adv. Chem. Ser.* **1979**, *173*, 162. (b) Chang, C. K. *J. Heterocycl. Chem.* **1977**, *14*, 1285. (c) Chang, C. K.; Kuo, M. S.; Wang, C. B. *J. Heterocycl. Chem.* **1977**, *14*, 943. (d) Chang, C. K. *J. Chem. Soc., Chem. Commun.* **1977**, 800.
(30) Rasha, M.; Rawls, H. R.; El Bayoumi, M. A. *Pure Appl. Chem.* **1965**, *11*, 371.

Table II. UV–Visible Spectrophotometric Data for the Neutral and Oxidized Forms of the Zinc Mono- and Diporphyrins in PhCN, 0.2 M Bu_4NPF_6: Soret/Visible Region [λ/nm ($10^{-3}\epsilon$/L mol^{-1} cm^{-1} ± 10%)]

porphyrin	neutral species	one-electron-oxidized species	two-electron-oxidized species
ZnTPP	425 (490)/553 (17.8), 594 (5.6)		409 (130)/600 (L) (9)
ZnC2diE	408 (380)/536 (20), 553 (21)		
Zn_2FTF6	401 (330)/534 (20), 569 (30)	330, 370, 400/533, 569, 650	366 (100)/536 (sh), 574 (13), 650 (2.5)
Zn_2FTF5 3-1	388 (320)/534 (16), 575 (22)	377 (120)/536 (7.2)	340 (104)/588 (9.3)
Zn_2FTF5 2-2	387 (340)/535 (14.5), 572 (20.8)	382 (135)/535 (9.2), 572 (9)	346 (98)/582 (11)
Zn_2FTF4	386 (290)/539 (10.5), 574 (16.5)	381 (135)/540 (7.7)	364 (100)/590 (8.5)
ZnMPA	414 (220)/540 (14), 574 (11)		
$Zn_2$1-5DPB	418/540, 574		
Zn_2DPA	405 (342)/531 (23), 571 (21)	383, 404 (160)/536 (14), 571 (13), 662 (8)	380 (90)/596 (9), 659 (13)
Zn_2DPB	391 (300)/545 (15), 578 (13)	382 (140)/540 (10), 670 (3.4)	364 (125)/608 (12.4)

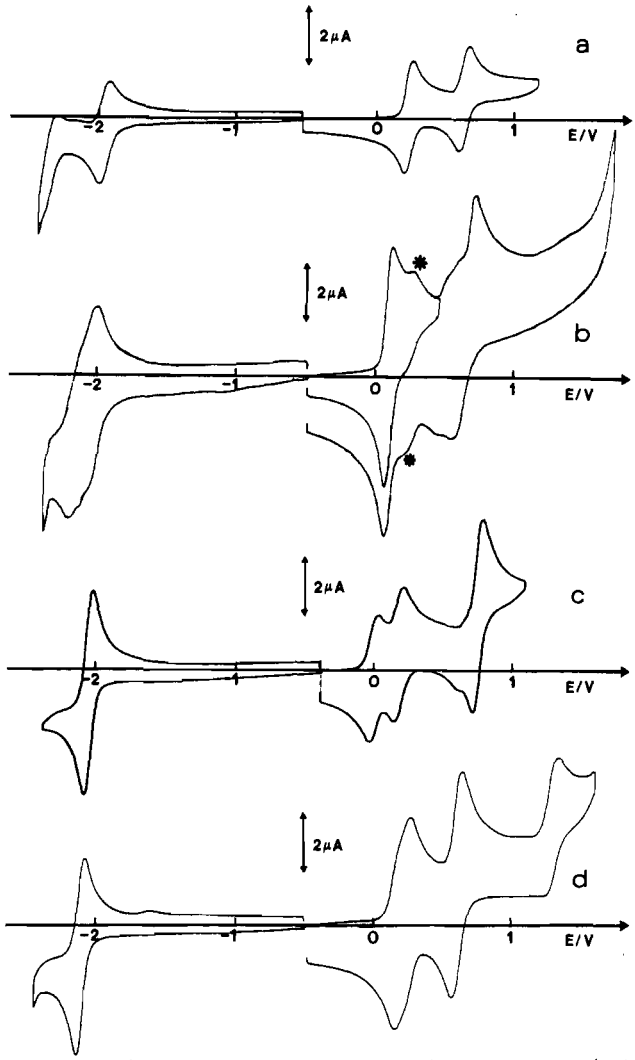

Figure 3. Cyclic voltammograms of the zinc porphyrins (ca. 4×10^{-4} M) in PhCN, 0.2 M Bu_4NPF_6 (platinum electrode; scan rate 0.1 V s^{-1}; vs Fc^+/Fc): (a) ZnC_2diE; (b) Zn_2FTF6; (c) Zn_2FTF4; (d) Zn_2DPA. Asterisks indicate peaks ascribed to an impurity in the Zn_2FTF6 sample.

not surprising considering the reactivity of the dicationic species.[25e] Moreover, in the case of the FTF5 dimers, the recorded values greater than 60 mV are, at least partially, ascribable to an unresolved splitting of this second redox process.

The above results (Table I) demonstrate that these two series of dimers give rise to an intricate redox situation. All of the different possible redox pathways observed here are gathered in Scheme II.

Each redox process (first or second oxidation, first reduction) either occurred by a two-electron step or was split into two one-electron steps. Some compounds gave no (or only slightly) split redox process, such as Zn_2FTF6 and Zn_2DPA (Figure 3, curves b and c), others like the two Zn_2FTF5 compounds (not shown) have all three of their processes split, or some exhibit only one split process, like Zn_2FTF4 (Figure 3, curve c) or have only

Scheme II. General Redox Pathway for the Oxidation or Reduction of the Cofacial Biporphyrin Rings[a]

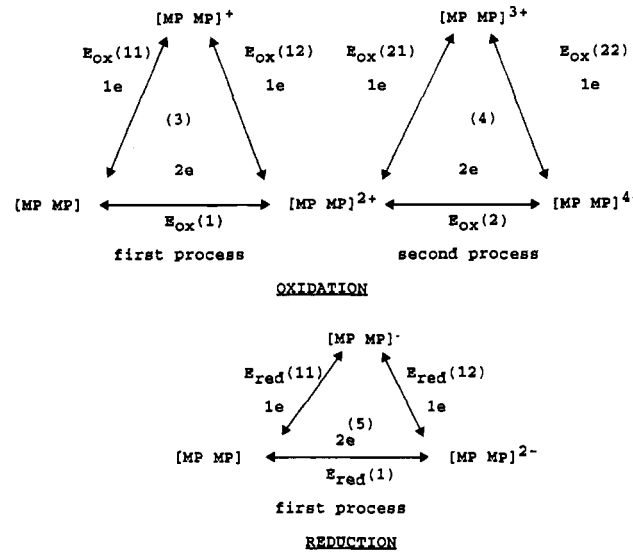

[a] P = porphyrin ring; M = nonelectroactive metal.

two split processes among the three. Interestingly, the offset dimer $Zn_2$1-5DPB does not show any split peaks but behaves just as a monomer; this demonstrates that the splitting is an interactive face-to-face process with no involvement of the aromatic bridge.

In an attempt to clarify the situation, only the first oxidation process was initially taken into account. This restricted viewpoint is justified below. If only this process is considered, it appears that the same classification of the dimers can be offered as that obtained previously in the case of the cobalt dimers.[21] When the two porphyrins are linked by the longest bridges, the so-called group 1 dimers FTF6 and DPA, the first two electrons are abstracted at the same or very close potentials (Figure 3b,d). If the inter-ring distance is shortened, group 2 compounds FTF4, FTF5 3-1, and FTF5 2-2, a large splitting of the first oxidation process into two one-electron steps is observed (Figure 3c). It thus became clear that the redox splitting in biporphyrins, observed for the first time with the cobalt derivatives, originates from cofacial interactions between the two π systems of the porphyrin rings and is not strictly related, as earlier postulated, to metal–metal interactions, which cannot be implicated in the case of these present exchanges. Furthermore, redox splitting is also observed in the case of the free-base (H_4) derivatives.

UV–Visible Spectroscopy. The effect of the proximity of the two rings on the π-cationic forms of these dimers was examined by the mean of their UV–vis spectra recorded, in their different redox states, either after an oxidation after each of the two one-electron steps for the group 2 dimers ([MP MP]$^+$ and [MP MP]$^{2+}$) or after a half-electrolysis and an exhaustive one at the potential of the two-electron step for the group 1 dimers. The typical spectra for the oxidized forms of porphyrins have been widely described[25,31] and shown to be dependent on the ground state, A_{2u} or A_{1u},[31,32] in the case of the π-cation radicals.

(31) Dolphin, D.; Felton, R. H. *Acc. Chem. Res.* **1974**, *7*, 26.

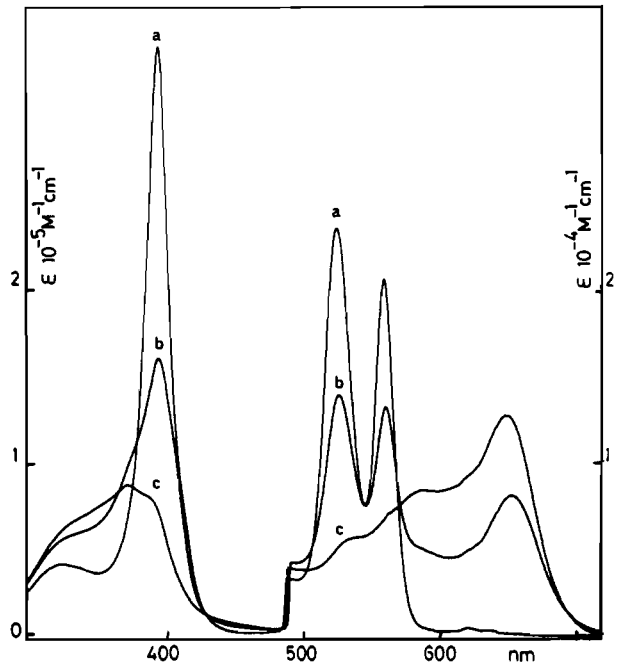

Figure 4. UV–visible spectra recorded during the oxidation of the Zn_2-DPA diporphyrin in PhCN, 0.2 M Bu_4NPF_6: (a) neutral form; (b) one-electron-oxidized form at 0.3 V (one electron per mole); (c) two-electron-oxidized form at 0.3 V.

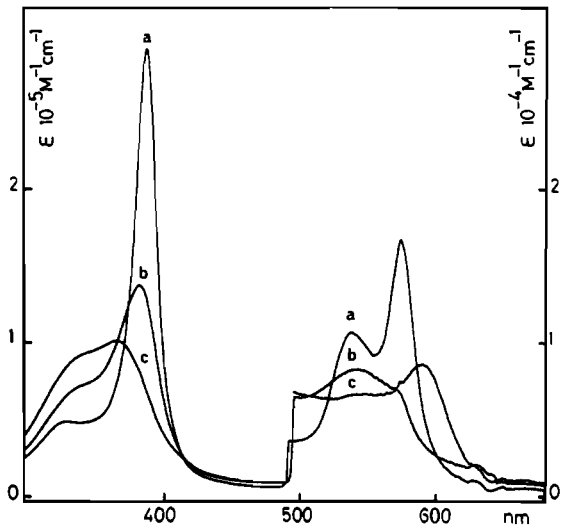

Figure 5. UV–visible spectra recorded during the oxidation of the Zn_2FTF4 diporphyrin in PhCN, 0.2 M Bu_4NPF_6: (a) neutral form; (b) one-electron-oxidized species (first wave, 0.1 V); (c) two-electron-oxidized species (second wave, 0.3 V).

The spectral data for the present zinc derivatives are reported in Table II, while the typical evolution of the spectra during oxidation for each group of dimers is shown in Figures 4 and 5. The spectra of the oxidized derivatives of some of the dicopper derivatives were also obtained but are not given here as they are not significantly different. An inspection of Table II shows that, in their neutral forms, these dimers display the usual blue shift of the Soret band, which is observed for highly conjugated porphyrin systems and which is due to exciton coupling.[15g,k,29,30]

The spectra obtained for the oxidized forms validate the classification of the dimers into two groups. From the evolution of the spectra of the group 1 dimers, shown in Figure 4 for Zn_2DPA, and qualitatively the same for Zn_2FTF6, it is evident that the half-oxidized solutions of these dimers are composed of a simple mixture of the initial neutral form and of the final two-electron-oxidized form. No specific feature ascribable to an intermediate species is seen on the half-oxidized-solution spectrum. The absence of isosbestic points in this set is due to the fact that the spectra were recorded from three different solutions. In the case of the group 2 dimers, exemplified in Figure 5 by the spectrum of Zn_2FTF4, it is evident, conversely, that the spectrum of the one-electron-oxidized species (curve b) is completely different from any combination of those of the neutral and dioxidized forms. The spectra are similar for all the other group 2 dimers (Table II). This is a strong indication that this monooxidized form $[MP\ MP]^+$ is totally different from the simple sum of a neutral and an oxidized form but can be best described as some "special", perhaps delocalized form. However, this spectrum, limited to the UV–visible domain, as well as those of the two-electron-oxidized forms of the group 2 dimers (curve c, Figure 5), does not show any specific feature ascribable to an intervalence transition that would reveal a delocalization process, and the near-IR domain has not been scrutinized yet. In addition to the group 1 dimers, the group 2 dimers display characteristics of monomeric π-cation radicals.[25,31]

Table III. EPR Data for the π-Cation Oxidized Forms of the Zinc Diporphyrins[a]

compd	charge	g	LW, G	I_H[b]	I_A[c]
ZnTPP	+	2.003_2	6.0	1	1
ZnC_2diE	+	2.002_9	5.9	0.01	
Zn_2FTF5 3-1	+	2.003_3	6.5	1	0.8
	2+	2.003_3	6.5	0.02	
Zn_2FTF5 2-2	+	2.002_9	5.9	0.9	0.6
	2+	2.002_9	5.9	0.05	
Zn_2FTF4	+	2.003	5.8	0.9	0.7
	2+	2.003	5.8	0.05	
Zn_2FTF6	+	2.002_9	6.0	0.25	0.2
	2+	2.002_9	6.0	0.5	0.4
Zn_2DPB	+	2.003	5.1	2.7	1.7
	2+	2.003	5.1	0.01	
Zn_2DPA	+	2.003	5.3	2.4	1.5
	2+	$[2.002_6$	6.5][d]		0.5

[a] In PhCN, 0.2 M Bu_4NPF_6, at 130 K; $C = 5 \times 10^{-4}$ M; power = 0.1 mW; modulation = 6.3 G. [b] I_H = integration value determined as the ratio of the peak height to that of $[ZnTPP^\bullet]^+$ per unit of concentration.[36] [c] I_A = integration value determined as the ratio of the geometrically measured peak area to that of $[ZnTPP^\bullet]^+$ per unit of concentration.[36] [d] g value for the central line of this spectrum; see text and Figure 7 regarding this spectrum.

EPR Spectroscopy. Although UV–vis spectroscopy and the analysis of the electrochemical data (vide infra) provide some support for the electronic configuration in the different forms of the dimers, they do not indicate with any certainty the electronic localization. In that connection, the EPR spectra of the zinc and copper derivatives in their different redox states were obtained and analyzed, both in shape and in intensity.

Zinc Derivatives. The neutral form of the zinc porphyrin derivatives is evidently diamagnetic owing to the d^{10} configuration of the metal. The ring-centered one-electron-oxidized form of porphyrin, so-called π-cation radical, gives rise to an EPR signal whose characteristics, largely discussed in the literature, can describe the delocalization of the electron on the different components of the ring and are thus also dependent on the ground state.[25b,d,32,33] In many cases however, aggregation reactions lead to the formation of dimers of these π-cations in which the two odd electrons become spin-paired, giving rise to a kind of π–π-bonded diamagnetic derivative:[34,35]

$$\downarrow[MP^\bullet]^+ + \downarrow[MP^\bullet]^+ \ <=====> \ [MP\overset{\downarrow\uparrow}{---}MP]^{2+} \qquad (6)$$

(32) Gouterman, M. In ref 12b, Vol. III, p 1.

(33) (a) Fajer, J.; Davis, M. S. In ref 12b, Vol. IV, p 197. (b) Fajer, J.; Borg, D. C.; Forman, A.; Felton, R. H.; Vegh, L.; Dolphin, D. *Ann. N.Y. Acad. Sci.* **1973**, *206*, 349.

(34) White, W. I. In ref 12b, Vol. V, p 303.

(35) (a) Song, H.; Reed, C. A.; Scheidt, W. R. *J. Am. Chem. Soc.* **1989**, *111*, 6867. (b) Fuhrhop, J. H.; Wasser, P.; Riesner, D.; Mauzerall, D. *J. Am. Chem. Soc.* **1972**, *94*, 7996. (c) Erler, B. S.; Scholz, W. F.; Lee, Y. J.; Scheidt, W. R.; Reed, C. A. *J. Am. Chem. Soc.* **1987**, *109*, 2644. (d) Godziela, G. M.; Goff, H. M. *J. Am. Chem. Soc.* **1986**, *108*, 2237. (e) Lemtur, A.; Chakravorty, B. K.; Subramanian, J. *J. Phys. Chem.* **1984**, *88*, 5603.

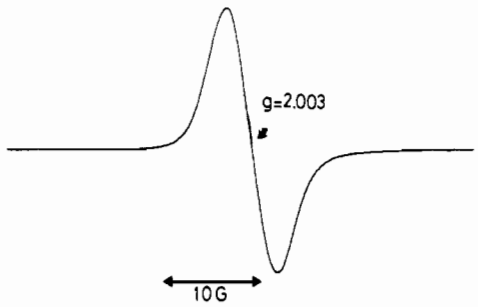

Figure 6. EPR one-line spectrum observed after a one-electron oxidation of a Zn_2FTF4 solution in PhCN, 0.2 M Bu_4NPF_6, frozen at 130 K.

This is the case with the ZnC2diE derivative; its one-electron oxidation yields a radical giving a single-line spectrum in frozen PhCN, Bu_4NPF_6, with $g = 2.003$ and LW (line width) = 5.9 G, but with an extremely low intensity. This unhindered derivative of the etioporphyrin (flat porphyrin) favors aggregation. Conversely, it is known that the π-cation of the highly hindered tetraphenylporphyrin does not give rise to association, especially in weakly polar solvents such as PhCN. In the present case, frozen PhCN, 0.1 M Bu_4NPF_6, the spectrum of $[ZnTPP^{\bullet}]^+$ is a single line with a normal intensity (see Table III). For that reason, the EPR signal of $[ZnTPP^{\bullet}]^+$ was chosen as a standard for integration of the EPR signals of the dimers. The integration was carried out in two different ways by use of either the height or the area of the peak. These values, in Table III, are expressed as their ratio to that obtained for $[ZnTPP^{\bullet}]^+$, under the same conditions.[36] The variation of the intensity of their signals as a function of their redox states was thus examined by following this procedure.

In the case of all the group 2 derivatives (Zn_2FTF4, Zn_2FTF5 2-2, Zn_2FTF5 3-1, and Zn_2DPB), the spectra obtained for the mono- and dioxidized forms are always very similar in shape to that depicted in Figure 6. It is a typical signal of a monoporphyrin π-cation radical. However, the integrated area for the monooxidized form is equal (or greater in the case of Zn_2DPB[36]) to unity, indicating that the π-cation is quantitatively formed, with no or little aggregation. This oxidized form can thus be described as a π-cation radical with one electron for two rings, but there is no indication of electronic delocalization, such as the previously proposed lowering of the line width as compared to that of a monomer[19h,29a,37] (Table III). Conversely, the integrated values obtained for the dioxidized derivatives of these group 2 dimers are nearly zero, except for a remaining impurity of the preceding species. This seems to indicate that in this dioxidized form the two virtually unpaired electrons of the dimer give rise to spin coupling, either intra- or intermolecular. The nonobservation of aggregation in the case of the monooxidized form is nevertheless an indication that the coupling is more likely to be intramolecular.

In the case of the group 1 dimers (FTF6 and DPA), for which the two electrons are simultaneously abstracted, the situation is different from that of the former group, but also differs for the two dimers Zn_2FTF6 and Zn_2DPA. When Zn_2FTF6 is oxidized, the EPR spectrum observed is a single line similar to that described above (cf. Table III and Figure 6); however, in this case, the intensity of the signal continues to increase from the beginning to the end of the two-electron oxidation. This situation is also different in that the intensity of the signal is much weaker than it should be. For example, as seen in Table III, for one equivalent electron abstracted the intensity is only $^1/_4$, whereas for two electrons abstracted it becomes $^1/_2$ of an equivalent-spin. This evidences a situation completely different from that of the group 2 dimers, as far as the spin coupling is concerned. Clearly, spin couplings are observed again, but once more these results do not reveal their nature, inter- or intramolecular.

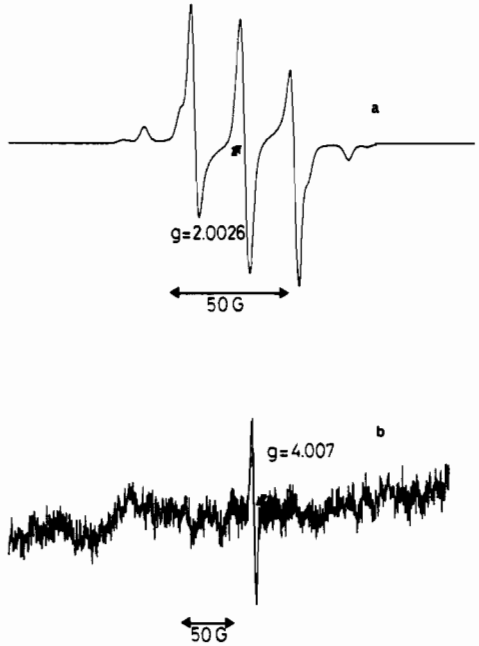

Figure 7. EPR spectrum of a two-electron-oxidized solution of Zn_2DPA at 130 K, in PhCN, 0.2 M Bu_4NPF_6: (a) full-field region; (b) enlarged half-field region.

In the case of the other member of group 1, Zn_2DPA, the one-electron-oxidized product displays an EPR spectrum, the intensity of which, compared with its Zn_2DPB homologue, indicates no spin coupling but an odd electron for two rings, as in the case of group 2 compounds.[36] However, the EPR signal obtained after an exhaustive two-electron electrolysis of this derivative was unexpected; it is shown in Figure 7. This spectrum was obtained under the same conditions as the others, frozen PhCN, Bu_4NPF_6, at 140 K; the solution is fairly stable over 1–2 h. It appears that the signal is the superposition of two spectra. One is the central line, while the other is composed of a set of several lines associated with a half-field transition line in the $g = 4$ region shown in Figure 7b. The intensities of these two spectra interconvert irreproducibly depending on the experiment or on the freshness of the electrolyzed solution. Actually, the latter spectrum of this signal corresponds to the typical signal obtained for a diradical in a triplet state.[38,39] This assignment is undoubtedly corroborated by the observation of the $\Delta m_s = 2$ line. As for the central line, it is similar to that of any porphyrin π-cation radical. The observation of such a double EPR signal is in fact somewhat common in the area of organic diradicals.[39] It is interpreted as due to association reactions between diradicals, especially at low temperature, which are actually very similar to the aggregation reactions between π-cations of porphyrins. This association, as shown in (7), is very likely to produce species which

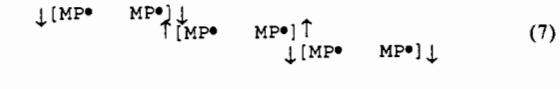

(7)

(36) As can be seen from Table III, the values derived from the heights of the peaks differ substantially from those obtained from the area in several instances. This can be explained by the fact that these "normalized" integration values are greatly dependent on the line width and shape of the signal. When the line shape and width are close to those of $[ZnTPP^{\bullet}]^+$, the integration values are satisfactory (FTF*n* series), whereas when the signal is much narrower than that of $[ZnTPP^{\bullet}]^+$ ("Pacman" DP series), values greater than unity are obtained: this of course does not mean that more than one unpaired electron is present in these monooxidized forms, only that the mechanical integration procedure is more efficient for this kind of signal. This is corroborated by the fact that the area-derived values are much better in the case of the DP series, which have a narrower signal. Nevertheless, these values remain indicative in the same series of compounds.

(37) (a) Norris, J. R.; Druyan, M. E.; Katz, J. J. *J. Am. Chem. Soc.* **1973**, *95*, 1680. (b) *J. Am. Chem. Soc.* **1973**, *95*, 1682. (c) Warden, J. T.; Bolton, J. R. *Acc. Chem. Res.* **1974**, *7*, 189.

(38) (a) Gordy, W. *Techniques of Chemistry*; Wiley: New York, 1980; Vol. XV, p 543. (b) Wasserman, E.; Hutton, R. S. *Acc. Chem. Res.* **1977**, *10*, 27.

(39) Ikegami, Y.; Muramatsu, T.; Hanaya, K.; Onodera, S.; Nakayama, N.; Kosower, E. M. *J. Am. Chem. Soc.* **1987**, *109*, 2876.

should have an average spectrum similar to that of a π-cation monomer, the spins of the stacked rings becoming paired two by two.[39] This interpretation accounts very well for the present observation, namely the two interconverting spectra and a very low integration value (Table III) resulting from the existence of three different electronic configurations: $S = 1$ (monomer in the triplet state), $S = {}^1/_2 + S = {}^1/_2$ (decoupled ending rings of the aggregated dimers), and $S = {}^1/_2 - {}^1/_2 = 0$ (neighboring aggregated paired rings). As a result, this spectrum clearly indicates that the oxidation of the Zn_2DPA yields a species which is formally a π-cation diradical, i.e. a derivative in which each ring bears an odd electron which is not too strongly coupled, and unpaired, with that of the other ring of the same dimer. An alternate interpretation would be the formation of the triplet from two independent rings, but this is very unlikely, as usually π-cation radicals give rise to diamagnetic dimers in the aggregates. This is the first time to our knowledge that in porphyrin chemistry the formation of a diradical in a triplet state is observed.

Although some interesting conclusions can be drawn out from the preceding results, it is still impossible to depict clearly the spin coupling between the two different groups of dimers owing to the possible existence of both intra- and intermolecular interactions.

Copper Derivatives. It is well-known that the EPR spectra of the π-cation derivatives of porphyrin with a paramagnetic metal center such as copper, iron, or vanadyl are usually somewhat complicated by the existence of intramolecular d–π coupling due to interaction of the two unpaired electrons, one on the metal and one on the ring, as well as d–d and π–π intermolecular couplings resulting from aggregation.[35c-e] In the present case, the possibility of aggregation between two or more of the already covalently linked dimers was likely to lead to an intricate spin situation. Nevertheless, we examined the EPR spectra of two typical copper derivatives of each group, Cu_2FTF5 3-1 for group 2 and Cu_2FTF6 for group 1, in their different redox states, as a last hope to be able to describe unambiguously the spin localization, by using the odd electrons on the copper atoms as a magnetic probe for those on the porphyrin rings.

In Figure 8 are shown the set of spectra obtained for the Cu2FTF5 3-1 group 2 dimer (curves b–d) as well as that of a Cu(II) monoporphyrin (curve a) for comparison. The latter clearly displays three out of the four lines of the parallel component, due to the hyperfine coupling with the copper atom ($I = {}^3/_2$), whereas the perpendicular gives one unresolved line.[40] In the case of Cu_2FTF5 3-1 in its neutral form, a quite different spectrum is observed (Figure 8b): this is the normal spectrum for such dimers with strong exchange-coupled copper systems.[35d,41] Both the perpendicular and parallel transitions are split; the latter one gives rise to the usual partially resolved seven hyperfine lines (two Cu atoms with $I = {}^3/_2$) on the left-hand high-field part of the spectrum. The forbidden transition $\Delta m_s = 2$ is also observed in the $g = 4$ region. The other dimers of group 2 give very similar spectra but with slightly different values of the zero-field-splitting parameter (ZFS), $D = 340 \times 10^{-4}$ cm^{-1} for FTF4 and FTF5 2-1 and $D = 360 \times 10^{-4}$ cm^{-1} for FTF5 3-1. This parameter is a measurement of the interactions between the two copper atoms and in many instances has been used to estimate the metal–metal distances;[41] the reported values were obtained by direct measurements on the spectra. After a one-electron oxidation of this compound, the spectrum of Figure 8c is obtained. It is completely different from that of a monomer (curve a), of a dimer (curve b), or of a π-cation (Figure 6), as well as of any combination of them. No $\Delta m_s = 2$ line is observed in the $g = 4$ region. It is in fact very reminiscent of those described for highly delocalized $S = {}^1/_2$ systems:[35d] the observation of such a spectrum is proposed to reflect the average magnetic situation in which, among the three virtual odd electrons (two on the copper atoms and one for the rings), two of them are spin-paired (no $\Delta m_s = 2$ line) whereas the third is delocalized over the whole dimer. Even though a theoretical interpretation of this spectrum is not available, such an assignment is corroborated by the subsequent spectrum. When Cu_2FTF5 3-1 is exhaustively oxidized by two electrons (second wave), the spectrum shown in Figure 8d is observed. This spectrum looks surprisingly like that of the initial neutral form (curve b) and is actually superimposable on it, in both the full- and the half-field region, as well having similar intensity. This indicates unambiguously that the two virtually odd electrons of the two rings are fully spin-paired, probably by delocalization over the two rings, and do not magnetically interact with those of the two coppers. Consequently, it can be deduced that the mutual geometric and magnetic situation of the two coppers remains the same whatever the oxidation state is. Therefore, this confirms the interpretation given for the intermediate spectrum (curve c, Figure 8) as that of a species in which the two coppers are still virtually interacting, but in fact alternatively coupling with the π-cationic odd electron totally delocalized over the two rings.

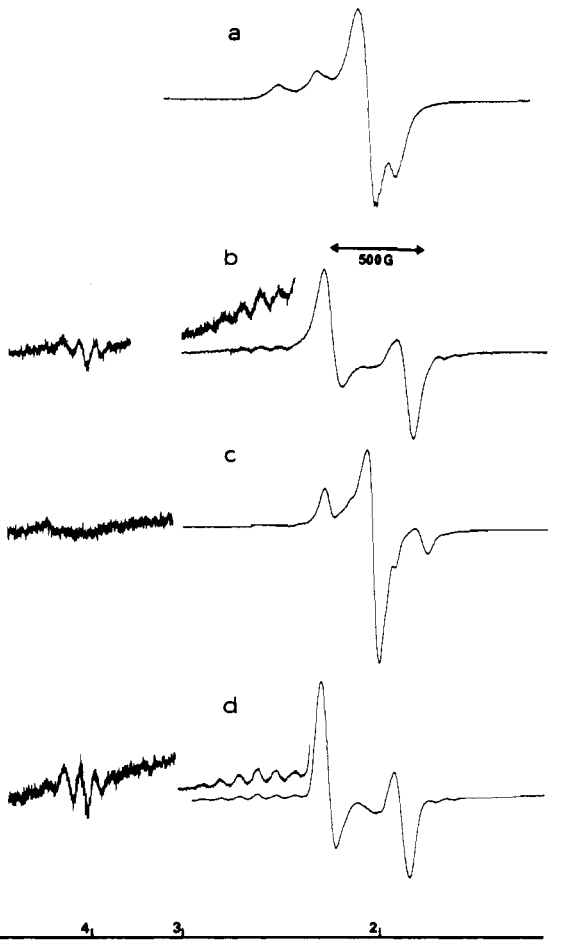

Figure 8. EPR spectra of copper porphyrins in frozen CH_2Cl_2, 0.2 M Bu_4NPF_6, at 130 K: (a) Cu(II) monoporphyrin; (b) Cu_2FTF5 3-1, neutral form; (c) $[Cu_2$FTF5 3-1$]^+$, one-electron-oxidized form (first wave); (d) $[Cu_2$FTF5 3-1$]^{2+}$, two-electron-oxidized form (second wave).

The situation in the case of the Cu_2FTF6 derivative, a group 1 compound, is illustrated by Figure 9. The initial neutral compound (curve a) displays a weakly intense spectrum, typical of a copper(II) monoporphyrin (see Figure 8, curve a), indicating that no or very weak exchange coupling exists in this compound. This is due to the longer linking bridges in this dimer. When the solution has been half-oxidized, i.e. when one electron per molecule, on the average, has been abstracted, unexpectedly a spectrum typical of the $S = {}^1/_2$ delocalized system of three virtual spins is again observed (Figure 9b). Even more surprising is the fact that when the Cu_2FTF6 compound has been totally oxidized by two electrons, a spectrum of a dicopper(II) system in a triplet state is observed, as shown in Figure 9c. Amazingly, the ZFS parameter D for this spectrum ($D = 400 \times 10^{-4}$ cm^{-1}) is even greater than that for any of the other tight dimers (vide supra). It thus appears

(40) Lin, W. C. In ref 12b, Vol. IV, p 358.
(41) Eaton, S. S.; Eaton, G. R.; Chang, C. K. *J. Am. Chem. Soc.* **1985**, *107*, 3177.

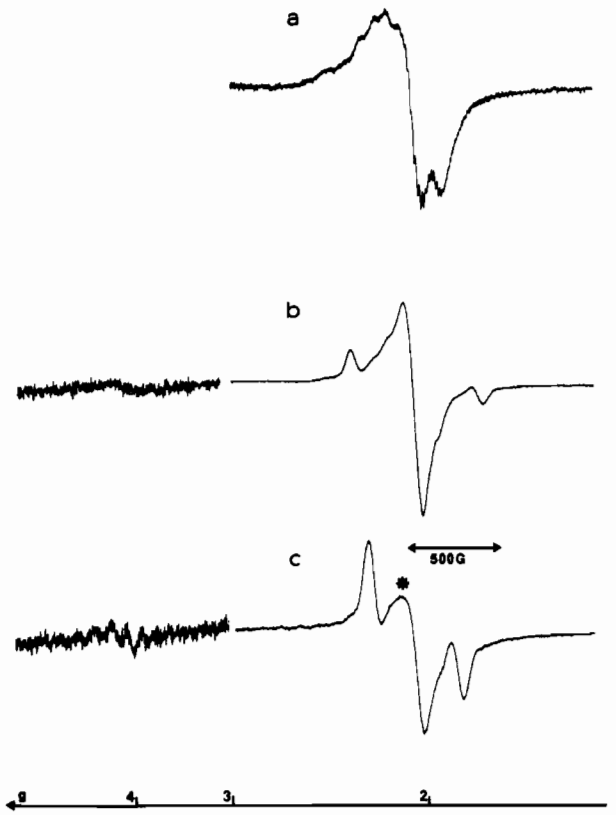

Figure 9. EPR spectra of Cu_2FTF6 diporphyrins in frozen CH_2Cl_2, 0.2 M Bu_4NPF_6, at 130 K: (a) neutral form; (b) one-electron-oxidized form; (c) two-electron-oxidized form. Asterisk indicates aggregation line.[41]

that even though no metal–metal interaction exists in the neutral form, as soon as one equivalent-electron per molecule of dimer has been abstracted, copper–copper interactions as well as π-cationic electron delocalization are observed. This leads back to the question of the nature, inter- (via aggregation) or intramolecular, of these couplings. For these to be intramolecular would require a structural rearrangement such that the copper–copper distance would become much smaller than in all the group 2 dimers, as indicated by the D values. For that, the only possibility would consist of a twisting of the two rings around the metal axis, which would require a significant stretching of the two amide bridges. This does not seem likely with respect to the only driving force of the reaction, which would be a kind of "intramolecular aggregation". Moreover, the present observations are very similar to others previously obtained with copper monoporphyrins:[35d] in that case, the same set of spectra as in Figure 9 have been obtained with the same aggregation line and approximately the same ZFS value, D, as those of spectrum c. These observations, thus, demonstrate that, in the case of the Cu_2FTF6 group 2 dimer, owing to the greater length of the linking bridge, the two copper porphyrins behave as independently as two monomers, formally equivalent to noncoupled diradicals. Indeed, these dimers give rise to intermolecular aggregation just as monomers do. This is consistent with the interpretation of the results obtained with the zinc derivatives.

Discussion

A brief overview of the preceding results allows one to conclude that, as was the case for cobalt compounds, the classification of the face-to-face diporphyrins into two groups is fully justified: namely one in which the two moieties are highly interactive, group 2, and the other, group 1, a borderline one in which the interporphyrin distance is such that the interactions tend to disappear. But, apart from this qualitative observation, a more quantitative and basic interpretation of the interactions can be gained from a careful analysis of these all results.

Analysis of the Electrochemical Data. Perusal of the redox potential values reported in Table I leads to some interesting

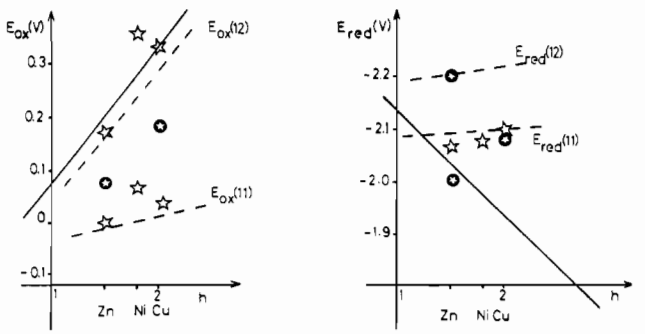

Figure 10. Influence of the electronegativity of the central ion on the oxidation and reduction potentials of the dimers. The electronegativity is expressed as the induction parameter, h, from Fuhrhop et al.[25a] The full straight lines are those obtained for a parent monoporphyrin, the octaethylporphyrin;[25a] the dashed lines stand for the mean variation of the redox potentials of the split redox processes, calculated as an average of the values obtained with all the group 2 dimers. Stars are for the case of the FTF4; black-circled stars, for the case of the FTF6.

observations. It has been widely demonstrated that the ring oxidation and reduction potentials for different metal derivatives of a given monoporphyrin are governed by the electronegativity of the central ion through an inductive effect:[24,25a,d,f] the more electronegative the ion, the more difficult the first oxidation and the easier the first reduction. Conversely, it is noteworthy from Table I that, for a given dimer of group 2 diporphyrins, the substitution of the central ion by another with a different electronegativity (e.g. Zn by Cu or Ni) has only a small and much less pronounced effect than in the case of the monomers. In order to understand this observation in a more comprehensive way, the redox potentials of the dimers are compared to those of the monomers in Figure 10. The full straight line represents the variation of $E_{ox}(1)$ and $E_{red}(2)$ obtained in the exemplary case of octaethylporphyrin: it corresponds to a plot of the first redox potentials $E_{ox}(1)$ and $E_{red}(1)$ obtained by Fuhrhop, Kadish, and Davis (reported here referenced to the Fc^+/Fc reference electrode) against the induction parameters h of the metal;[25a] the slopes of these lines reflect the effect of the electronegativity of the central ion on the redox potentials. The redox potentials of the C_2diE derivatives lie on these lines too, as this derivative of the etioporphyrin is not very different from OEP. These full lines are therefore a good comparison for the present dimers. The average variations for the redox potentials of all the group 2 dimers are denoted by the dashed lines in Figure 10. Exemplified by the stars are the points for the FTF4 derivatives, while the black-circled stars are those obtained in the case of the FTF6 group 1 dimer. This figure emphasizes the huge effect of the dimeric structure on the redox potentials: (i) it induces an important lowering of the first oxidation $E_{ox}(11)$ and of both reduction potentials $E_{red}(11)$ and $E_{red}(12)$ as compared to monomers; (ii) the electronegativity of the central ion has no effect on the first oxidation potential nor on the reduction potentials, as indicated by the quasi-parallelism of the corresponding dashed lines with the electronegativity axis. Conversely, the second oxidation step of the first oxidation process for the group 2 dimers ($E_{ox}(12)$) follows a trend similar to that of the monomer, whereas the group 1 dimer seems to display intermediate behavior regarding oxidation, closer to that of a monomer.

These observations suggest that the structural "biporphyrin effect" induces a repulsive electronic effect in the dimer in its neutral form, so important that the effect of the electronegativity of the central ion is lessened. An alternative explanation for this could be a "face-to-face" steric effect, such as hindrance to solvation; however, it has been shown that the nature and donor number of a solvent have little effect on the ring oxidation processes in the case of zinc porphyrins.[25c] Moreover, such a steric effect would not account for the differences between the dimers, whose solvent interactions are not likely to be different.

As a matter of fact, an indication that these special properties originate from interactions intrinsic only to these molecules can be borne out by another analysis of the potentials. In the case

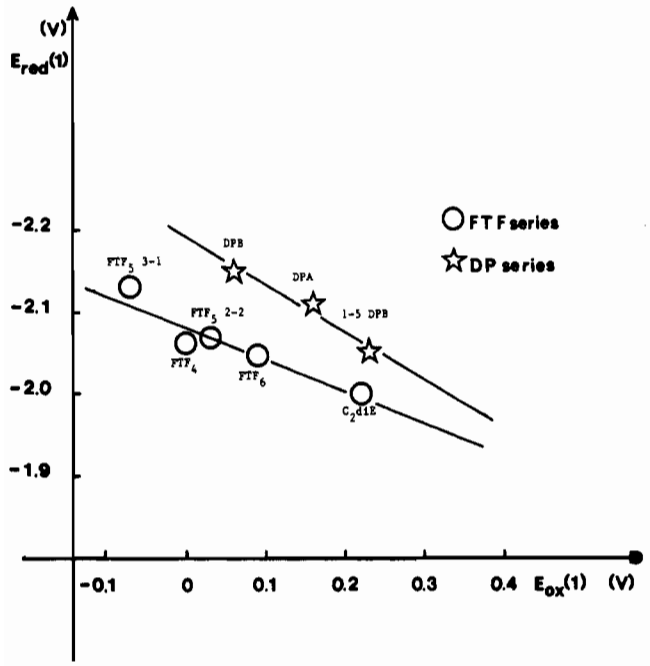

Figure 11. Variation of the first oxidation potential $E_{ox}(11)$ (or $E_{ox}(1)$) with the first reduction potential $E_{red}(11)$ (or $E_{red}(1)$), exemplifying the electronegativity/structure relationship for the dimeric ligands.

of a given monoporphyrin, when the electronegativity of the central ion is changed, a correlation is found between the first oxidation potential $E_{ox}(1)$ and first reduction potential $E_{red}(1)$, reflecting the induction effect: the more difficult the ring is to oxidize, the easier it is to reduce, and vice versa.[25a] In the present case, when for a given dimer the central ion is changed, no such correlation is found, neither between the first oxidation potential $E_{ox}(11)$ and the second reduction potential $E_{red}(12)$ nor between the second oxidation potential $E_{ox}(12)$ and first reduction potential $E_{red}(11)$, which would be the theoretical equivalent correlation for two independent rings in a dimer. As exemplified in Figure 11, if the potential of the first reduction step $E_{red}(11)$ (or $E_{red}(1)$) is plotted against the first oxidation step potential $E_{ox}(11)$ (or $E_{ox}(1)$) for the derivatives of the same metal (zinc in the present case) of the two series, FTF and Pacman, a linear correlation is observed. In the case of copper, a slightly poorer linearity is also observed. This demonstrates that (i) these dimers cannot be considered as two independent rings from a redox viewpoint, but as a single entity from (or to) which electrons are abstracted (or added), which implies an electronic delocalization process, and (ii) the enhancement of the electronic density in the neutral form of the dimers, as compared to the monomers, resulting from Coulomb repulsion is ascribable to and governed by the structure of the dimeric ligand itself, the metal ion having almost no effect. Accordingly, the points corresponding to the monomer-like compounds, C_2diE and 1-5 DPB, equivalent single redox entities in which the electronic Coulomb repulsion is zero, can be considered as the zero points for this correlation, and they consequently appear on the lowest part of the lines.

Actually, Figure 11 allows a classification of the dimers of the two series with regard to their electronic density. The so-obtained decreasing order is

FTF5 3-1 > FTF4 > FTF5 2-2 >FTF6 > C_2diE

and

DPB > DPA > 1-5 DPB

Interestingly, it appears that this order parallels exactly that obtained from the values of the split redox potentials for the first oxidation process: $\Delta E_{ox} = E_{ox}(12) - E_{ox}(11)$ shown in Table IV. For a given metal (Zn or Cu), the greater the electron repulsion, the greater ΔE_{ox}. For the two series of dimers, a quasi-linear relationship (not shown) is found between ΔE_{ox} and $E_{ox}(11)$ or

Table IV. Values of the Redox Splitting for the Oxidation and Reduction Ring Processes (mV)[a]

	$\Delta E_{ox} = E_{ox}(12) - E_{ox}(11)$				$\Delta E_{red} = E_{red}(11) - E_{red}(12)$			
ligand	Zn	Cu	H_2	Co(III)/Co(II)[b]	Zn	Cu	H_2	Co(II)/Co(I)
FTF6	0	0		0	150	0		0
DPA	70		120	0	0		0	0
FTF5 2-2	100	220		170	110	165		410
FTF5 3-1	190	310		245	100	110		390
FTF4	170	290	230	210	0	0	360	260
DPB	150			170	0			300

[a] Obtained from Table I and from ref 21 for cobalt compounds. [b] Formal redox states previously proposed[21] for the first oxidation process for cobalt compounds.

Scheme III. Formal Description Proposed for the One-Step First Oxidation Process of the Group 1 Diporphyrins with a Nonactive Metal Center[a]

$$[MP\quad MP] \xleftrightarrow[E_{ox}(1)]{-2e} [MP^{\bullet}\quad MP^{\bullet}]^{2+}$$

[a] • = unpaired electron.

Scheme IV. Formal Description of the Two-Step First Oxidation Process of the Rings in the Case of the Group 2 Diporphyrins[a]

$$[MP\quad MP] \xleftrightarrow[E_{ox}(11)]{-1e} [MP^{\bullet}\ MP]^{+} \xleftrightarrow[E_{ox}(12)]{-1e} [MP\text{---}MP]^{2+}$$

[a] • = unpaired electron delocalized over the two rings. --- = π–π bond between the two rings resulting from the pairing of the two delocalized electrons.

$E_{red}(11)$. This is not true for $\Delta E_{red} = E_{red}(11) - E_{red}(12)$, which does not seem to follow any interpretable trend. As a result, these considerations demonstrate that ΔE_{ox} (but not ΔE_{red}) is another comparative measurement of the electron density and thus of the interactions in these dimers. A retroinspection of Figure 10 affords an explanation of that fact. In the case of the group 2 dimers, it has been demonstrated that $E_{ox}(11)$ is independent of the central ion but is determined by the structure of the dimers. As soon as one electron has been abstracted, the dimers behave just like monomers, as exemplified by the parallel behavior and proximity of the dashed ($E_{ox}(12)$ for dimers) and full ($E_{ox}(1)$ for monomers) lines. Thus, it seems that the extra-electron density in the dimers is cancelled by the first electron removal, while the remaining electron delocalized over the two rings makes the two rings closer to a monomer in terms of electronic charge. In the case of the group 1 dimer FTF6, Figure 10 shows that the electronic density is a little modified but not enough to split the redox peaks and to lessen the inductive effect of the central ion on the redox potentials. It is quite evident that such an interpretation is not applicable to the reduction processes: in this case, the two successive electron transfers induce an increase of the π-ring repulsive interactions in the dimers, making them more and more difficult to reduce as compared to monomers, as is reflected by Figure 10, curve b. It is thus more hazardous to interpret the reduction behavior, but this demonstrates that as postulated above, the split oxidation is a good criterion for the classification of the dimers into two groups.

Description of the Oxidation Process. All the electrochemical and spectroscopic (UV–vis and EPR) results and the analysis concur to demonstrate the following descriptions for the oxidation processes of dimeric face-to-face porphyrins (Schemes III and IV).

When the two rings are far enough apart, the resulting group 1 dimers behave as the simple juxtaposition of two nearly noninteracting monomers. The two rings are simultaneously oxidized, yielding a species equivalent to a π-cation diradical.

This species does not display any spectroscopic (UV–vis) feature characteristically different from other π-cations. EPR spectroscopy shows that these species, like the monomers, readily give rise to intermolecular association with spin coupling. EPR spectra

of the FTF6 series are not very different from those of monomers. The formality of this description is especially emphasized by the observation of a triplet-state spectrum of a π-cation diradical of porphyrin: it is noteworthy that it is the first time that such a species has been observed in the chemistry of porphyrins. The fact that the triplet state is observed in the case of DPA, and not FTF6, could result from the steric hindrance of the anthracene moiety, which impedes aggregation; this is corroborated by the fact that the monooxidized species has a spectrum with an intensity of 1. Moreover, this kind of exchange interaction is likely to be transmitted by the orthogonal anthracene bridge.

When the two rings are very close to each other, the resulting so-called group 2 dimers display properties decidedly different from that of any summation of monomers. The electron distribution of the dimer is greatly modified as compared to that of the monomer, and the first oxidation process proceeds through two single electronic steps represented in Scheme IV.

The resulting unpaired electrons are delocalized over these two rings, giving rise in the first step to a completely delocalized π-cation radical and in the second oxidation step to the formation of a kind of $\pi-\pi$ bond between the two rings by total pairing of the two delocalized electrons. This kind of bond has already been proposed and discussed previously in the case of aggregation of π-cations of monoporphyrins,[35] but this is the first time it has been clearly observed by several means. As opposed to previous works, it is surprising that no characteristic spectral features could be observed for these oxidized species. The formation of such a bond has been proposed to be associated with the appearance of a new UV–vis band in the 900-nm region.[35b] The spectra of all the monooxidized delocalized π-cation radicals (FTF and Pacman series, Zn and Cu derivatives) share common features which seem specific to that redox state: a Soret band around 370 nm with a decreased intensity and a broad visible band near 540 nm (see Figure 5). Interestingly, these features are shared with their homologous cobalt derivatives[21] as well. Others have proposed that such delocalization of the odd electron over two rings, as in the case of chlorophyll, induces a decrease of the EPR line width,[19h,29a,37] but this is not observed here.

Structure/Interaction Relationship. Once classification and ordering of the interactions in these two series of dimers are in hand, the origin as well as the relationship between their intensity and the structure of these dimers remains to be explained. For that purpose, we examined structural data, molecular models, and other physicochemical data widespread in the literature concerning these or very similar compounds. Much literature is emerging concerning such $\pi-\pi$ interactions, with regard to both their nature and geometric requirements. Two pertinent reviews by Scheidt and Lee[42] and Sanders et al.[15h] have recently appeared. However, so far, in most cases it is the $\pi-\pi$ interactions that define the packing and geometry of the dimers, while here it is the linking bridges which define them, provided they are not too loose. This has proven to be true for most of the dimers studied here, and at least for the group 2 ones they are all related to the strongly interacting S group of Scheidt and Lee[42] and lie in the repulsion region of the Sanders diagram.[15h] Therefore, in the present case, we are examining the variation of the intensity of the interactions inside this category of highly interacting dimers. However, it must be kept in mind that the interactions previously described by these authors concerned dimers in a given redox state, i.e. in the neutral or oxidized π-cationic form; in the present case, the observations are based on the variations of the redox potentials with structure and thus account for the modifications of the internal interactions when the redox state of a dimer is changed.

The results and discussion presented above lead to the conclusion that the metal–metal interaction and a possible steric protecting effect created by the interporphyrin cavity do not play any role, or very minor, in the existence and intensity of the interactions. This is strongly corroborated if one looks at another property of the face-to-face dimers: the NMR upfield shifts of the internal pyrrole NH protons (δ(NH)) of the free-base derivatives. This shift is a well-known shielding effect due to the ring current interactions when the two moieties of a cofacial dimer are very closely spaced in a cofacial configuration.[13,26,39] The δ(NH) values for the two series of dimers studied in the present work, FTF*n*[13b,d,e] and DPX,[26] were collected from the literature and are gathered in Table V. The data of the Chang DP*n* series[29b,41] (very close to those of the Collman FTF*n* series) are also presented for the sake of discussion, as more structural data are available for this DP series. Interestingly, it appears that the order of the upfield δ(NH) shift for the two series, FTF and Pacman, is exactly the same as that derived from the electrochemical measurements, as well as from the EPR spectra of the dicopper derivatives, although the methods reflect very different physicochemical properties. This is particularly striking in the case of the two FTF5 and FTF4 dimers: while the three of them are highly interacting, the interactions are the most intense in the case of the FTF5 3-1 dimer, even though it has longer linking bridges than the FTF4. Moreover, this classification is independent of the central ion: free base, zinc, copper, and even cobalt.[21c,d] This last argument (NMR) points out that only the interactions between the two π systems govern the interactive process in the dimer; those between the two metal centers, albeit clearly existing, do not seem to have any effect on their extent. In another connection, this seems to indicate that the interactive process in the neutral form is the dominating one among those existing in the three redox forms.

This leads to questions about the structural and geometric factors that modulate the amplitude of the $\pi-\pi$ interactions. For that purpose, it is necessary to examine the available structural data,[41,43,44] which are unfortunately scarce, and subsequently CPK molecular models. In the discussion, the geometric parameters used are those shown in Figure 12. They are similar to those defined by Scheidt and Lee[42] when classifying $\pi-\pi$ interactions in stacked dimers. These are the lateral shift, LS, displacement between the two centers of the rings, the interplanar separation, IS, taken perpendicular to the ring planes, the shift angle, θ,

Table V. ^{1}H NMR Chemical Shifts for Internal Pyrrole Protons of Free-Base Porphyrin Monomers and Dimers Collected from the Literature[a]

	δ(NH)		δ(NH)
FTF series		DPN series	
H_2C2diE	−3.75[13b,d,e]		
		H4DP7	−6.2[29b]
H_4FTF6	−6.1[13b,d,e]	H4DP6	−6.6[29b]
H_4FTF5 2-2	−7.9[13b,d,e]	H4DP5	−8.5[29b]
H_4FTF5 3-1	−8.2[13b,d,e]		
H_4FTF4	−8.1[13b,d,e]	H4DP4	−7.9[41]
Pacman series			
H_2MPA	−2.55[26]		
H_4DPA	−5.0[26]		
H_4DPB	−7.5[26]		

[a] The DPN series has been synthesized and studied by Chang et al., and its derivatives are structurally quite close to those of the FTF series.

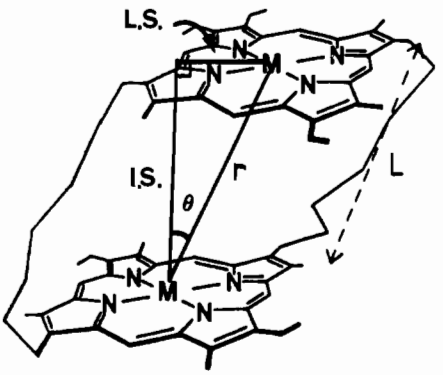

Figure 12. Illustration of the different structural factors defining the extent of the internal interactions: *r*, metal–metal distance; ID, interplanar distance, LS, lateral shift; θ, slip angle; L, linking bridge length, usually expressed by the number of constituting atoms.

(42) Scheidt, W. R.; Lee, Y. J. *Struct. Bonding (Berlin)* **1987**, *64*, 1.

Table VI. Structural Data for Copper Cofacial Diporphyrins Collected from the Literature

ligand	r, Å	θ, deg	IS, Å
DP7[a]	5.22 (5.0)	(40)	3.52 (3.8)
DP5[a]	(4.5)	(20)	(3.9)
FTF4[b]	3.42	2.2	3.54
DP4[a]	(4.04)	(15)	(4.0)
DPA	4.57 (4.9)	(30)	3.9 (4.6)
DPB	3.81 (4.14)	(20)	3.5 (3.9)

[a] Crystal structural data were obtained by Chang et al. Values in parentheses are the corresponding values obtained from an EPR analysis. r = metal–metal distance; θ = relative slipping angle of the two rings; IS = interplanar separation between the two rings.[41,44] [b] Crystal structural data.[43]

between IS and r, the metal–metal distance, and finally L, the linking bridge length. The structural data are collected in Table VI: most of them have been obtained from EPR calculations by Eaton, Eaton, and Chang[41] and are given in parentheses; those obtained by X-ray analysis[43,44] of crystals are more accurate.

Given the demonstrated $\pi-\pi$ origin of the interactions and ineffectiveness of the metal–metal ones, it is evident now that the metal–metal distance, r, is no longer the appropriate factor to be considered. The lateral shift and interplanar separation are more representative to define the overlap of the two π systems. These are the parameters also chosen by Scheidt and Lee,[42] who showed that the lateral shift has a preponderant effect: strong interactions require a small lateral shift, as long as the interplanar distance is not too large. As for the present diporphyrins, these criteria also seem to apply. In the case of DPA, although a greater interplanar separation exists, owing to the smaller lateral shift (lower value of θ), the overlap of the two π systems is more significant than for DP7, very close to the case of FTF6, in which LS and θ are important. This accounts for the slight redox splitting recorded in the case of DPA ($\Delta E_{ox} < 70$ mV), while in the case of FTF6 it is negligible.

In the case of the strongly interactive dimers of group 2, the situation is more puzzling. Our EPR measurements as well as those reported by Eaton, Eaton, and Chang[41] indicate a very short metal–metal distance with very small lateral shift and slip angle. This has been confirmed by the recent crystallographic data, for FTF4 and DPB (see Table VI). However this cannot explain why one of these dimers with a longer linking bridge length, FTF5 3-1, displays the most intense interactive behavior. Unfortunately in the case of FTF5 3-1 and FTF5 2-2, no crystallographic data are available, and the EPR data available for the cobalt or copper compounds are not interpretable. Thus, we made use of molecular models (CPK) to try to understand the situation.

Examination of molecular models in the case of the FTF4 dimer shows a very tight cofacial geometry of the two macrocyclic rings with regard to each other. This is due to the shortness and rigidity induced by the amide function and is in full agreement with the structure described by Kim, Collman, and Ibers.[43] In the case of FTF6, the presence of an extra $-CH_2-$ on each side of the amide function induces a high flexibility in the linking bridges, which allows a configuration with a very large lateral slippage and a very short interplanar distance, or the converse. The models we studied for the two FTF5 dimers showed that the addition of one more $-CH_2-$ groups on the lateral bridges, as compared to the case of the FTF4 dimer, induces a slight increase in r and IS but allows slippages of the two rings to take place owing to the greater flexibility. These lateral slippages seem to remain very small however, as the amide function is kept very close to one of the two rings. Therefore, the greater interactive behavior recorded, in the case of the FTF5 3-1 dimer, could result from a very slight increase in LS inducing a small IS, as compared to the case of both FTF4 and FTF5 2-2; this could likely be favorable to a better

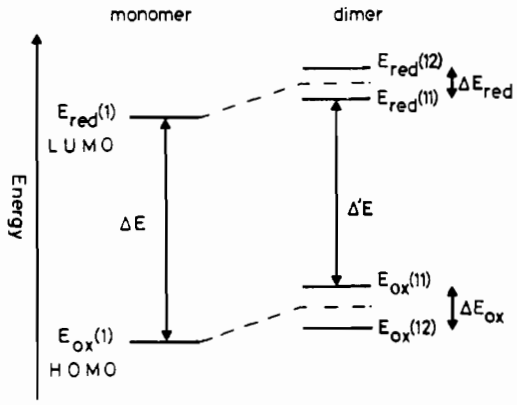

Figure 13. Qualitative diagram for the average influence of the dimeric structure on the redox potential behavior for the first oxidation and reduction processes.

overlap of the two π systems, increasing the interactive process. In another respect, the molecular models suggest that the central location of the amide carbonyl (C=O) function in the FTF5 3-1 bridge would induce greater rigidity in the chain, as compared to the case of the FTF5 2-2 dimer, which is likely to exhibit even more slippage. This proposal is corroborated by the EPR structural values obtained by Eaton, Eaton, and Chang for DP4 and DP5[41] (Table VI). Our results regarding the structural constraints necessary for the interactions to take place, based on the electrochemical measurements of their extent and corroborated by other methods, seem therefore to be in general agreement with the propositions of Scheidt and Lee[42] and Sanders et al.[15h] But these demonstrate that more subtle modulations of the configuration, namely a very slight increase of the lateral slippage with an increase of the metal–metal distance, can induce a decrease in the interplanar separation and greater interaction.

The differences between the two series, FTF and Pacman, seem difficult to interpret. FTF4 and DPB display similar behaviors, but their structural data are markedly different. Worthy of notice is that the metal–metal and interplanar distances are much greater in the case of DPB. However, it must be kept in mind that the linking bridges of the two series are different in several respects: (i) the aromatic character of the pillared links could help transmit the interaction through a π conjugation; (ii) the single link in the Pacman series could explain why the structural data are not the same in the solid crystalline state and in solution, by virtue of the so-called "Pacman effect" of the flexibility of the inter-ring cavity.

As a conclusion, it is now quite evident that the chemical nature of the linking bridge, more than just the length, will be the determining factor for the existence and modulation of the interactive processes defining the exact geometry of the dimers. This is in accordance with the fact that such processes were not recorded for most of the cofacial porphyrins studied so far:[19] they bear, in most cases, very long linking bridges or, in some instances, very short highly flexible bridges. This is the case for the $[-(CH_2)_4-]$ dibridged dimer synthesized by both Dolphin[19a] and Collman:[19f] it is noteworthy that this complex does not display either the UV–visible blue-shifted Soret band or NMR upfield-shifted pyrrolic protons (δ(NH)). Moreover, the present results are in good accordance with those recently presented for related cofacial diphthalocyanines.[16e]

Toward a Model for the $\pi-\pi$ Interactions. In light of the physical description of the $\pi-\pi$ interactions obtained from this study, it is possible to propose a qualitative electronic model accounting for their origin. In Figure 13 is displayed the average influence of the dimerization on the redox behavior for the first oxidation and reduction processes derived from Table I. The potential differences $\Delta E = E_{ox}(1) - E_{red}(1)$ are usually associated with the HOMO/LUMO energy gap of the porphyrin rings, when no redox metal exchange is involved. When one considers this diagram, it should be recalled that, in the highly interactive group 2 dimers, each of these first redox processes splits into two steps. It is noteworthy that the potential differences for the average

(43) Kim, K.; Collman, J. P.; Ibers, J. A. *J. Am. Chem. Soc.* **1988**, *110*, 4242.
(44) (a) Hatada, M. H.; Tulinsky, A.; Chang, C. K. *J. Am. Chem. Soc.* **1980**, *102*, 7115. (b) Fillers, J. P.; Ravichandran, K. G.; Abdalmuhdi, I.; Tulinsky, A.; Chang, C. K. *J. Am. Chem. Soc.* **1986**, *108*, 417.

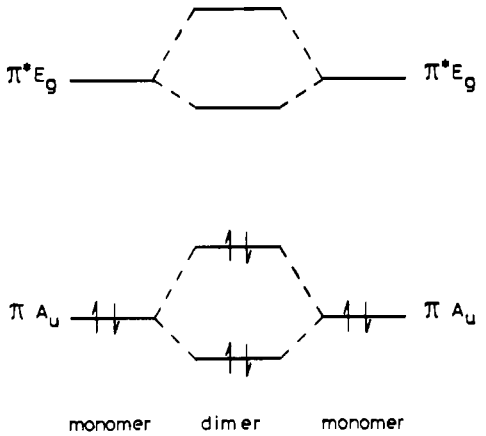

Figure 14. Qualitative molecular orbital diagram accounting for the observed redox interactive behavior of the porphyrin dimers.

potentials of the two one-electron oxidation and reduction processes (represented by dashed lines in the diagram)

$$\Delta E = [E_{ox}(12) - E_{ox}(11)]/2 - [E_{red}(12) - E_{red}(11)]/2 = E_{ox}(1) - E_{ox}(2)$$

remain constant for all the dimers and are equal to 2.25 ± 0.1 V (see Table I), which is the common value recorded for porphyrin monomers.[24b,25a,b,e,f] This of course only reflects the conservation of energy after dimerization but does not indicate, as others have observed in the case of less strongly interacting but dissymmetric dimers, that two sets of HOMO and LUMO are present.[15e] Since it has been proved that the present dimers constitute a single entity from a redox viewpoint, the HOMO/LUMO energy gap is now associated with the difference between the first oxidation and first reduction processes:

$$\Delta' E = E_{ox}(11) - E_{red}(11)$$

Thus another property of these dimers is a significant decrease in the HOMO/LUMO energy gap as compared to that of monomers ($\Delta' E_{dimer} - \Delta E_{monomer}$ = 80–160 mV), due to the lowering of the first oxidation potential by 200–300 mV and of the first reduction potential by 50–130 mV.

These observations can be tentatively interpreted in terms of the qualitative molecular orbital perturbation diagram shown in Figure 14. For the neutral form of the monomers, the two A_u π levels are filled; the resulting form of the dimers has both A_u π bonding and antibonding orbitals occupied. This induces a nonbonding interaction between the two rings through a highly repulsive effect and destabilization of the HOMO, leading to easier oxidation. In the monooxidized state, one electron has been removed from an antibonding level and the interaction gains bonding character, emphasized by the total delocalization of the spin over the two rings evidenced here. Accordingly, this level is stabilized and the second electron is more difficult to abstract [$E_{ox}(12) \ll E_{ox}(11)$]. In the dioxidized level, the two remaining π electrons are spin-paired in the bonding level, leading to bond formation between the two rings, which has been pointed out above. As a result, in this latter form, the dimers are stabilized as compared to radical π-cations of monomers: this is reflected in the increase of the potentials for the second oxidation process, $E_{ox}(2)$, observable in Table I ($\Delta E_{ox}(2)$ = 120 mV for zinc derivatives). This description affords theoretical support for the formation of the weak π–π nonclassical bond through dimerization of π-cation radicals.[35] In another connection, the MO diagram also exemplifies the decrease in the π–π^* HOMO/LUMO energy gap of the dimers (Figure 14).

As far as the reduction processes and thus the empty LUMO level are concerned, the situation remains more confused, as the successive electron additions induce growing interactive processes in the dimers and thus an increase in the differences of the electronic configurations as compared to the case of the monomers. Nonetheless, the decrease in the first reduction potential can be explained by stabilization of the first π^* level; the less pronounced decrease as compared to the case of oxidation could be the result of the initial vacancy of these orbitals. The following reduction step is likely to increase again the interactions and electron repulsion in the dimers, and this second step is thus very difficult and the potential behavior much farther from that of a monomer. This behavior is the opposite of oxidation, where the decrease of the electron density by electron removal renders the dimers closer to the monomers in terms of redox potentials.

Finally, the observation of peak to peak separations less than 60 mV in two cases (oxidation of Zn_2FTF6 and reduction of Zn_2FTF4; see Table I) can also be understood in terms of the same model. In such cases, it can be imagined that, through a special geometric configuration, the spin-paired bonding interaction created by the second oxidation (or second reduction) is so significant as compared to the one-electron delocalized case that this second electron exchange becomes thermodynamically easier than the first one.

Concluding Comments. The present results on the electrochemical behavior of diporphyrins complexed with a nonelectroactive metal, fully corroborated by spectroscopic data, demonstrate the existence of strong electronic π–π interactions between the two porphyrin rings and that they prevail over the metal–metal interactions. The interactive processes, in their type and extent, are defined by the mutual configuration of the halves of the dimer fixed by the nature and length of the linking bridge. An analysis of these data allows one to interpret these interactions in terms of an electronic perturbation diagram which is in complete agreement with the work of others who have applied different physicochemical methods to relevant systems such as very close face to face "Pacman" models of phthalocyanines,[16c] chlorophyll "special pair",[5a,9a] stacked silicon phthalocyanines,[17c] lanthanide sandwich porphyrins,[18] .... This diagram is an argument for these dimers to be considered as new single entities[35a,b] from a redox standpoint. In another connection, it affords an explanation of many properties of these compounds and similar ones, synthetic or natural, involved in electron-transfer reactions. Particularly striking in this area are observations especially relevant to these processes, such as lowering of the oxidation potentials associated with a decrease in the HOMO/LUMO energy gap (both supposed capable of easing the primary step-photoejection of photosystem I)[10,15b,c,16e,17b–c,18e,19d,e,h] as well as electronic delocalization processes in π-cationic forms, a π-cation diradical in a triplet state, and formation of the nonclassical π–π bond between the two rings.[6,15i,19h,29a,35,37]

As far as our first goal is concerned, which was to understand the four-electron catalytic O_2 reduction mediated by the dicobalt derivatives of these dimers, the present findings do not afford new clues a priori. The classification into two groups is exactly the same as that obtained with the cobalt derivatives[21] and thus still does not parallel the efficiency of these dimers with regard to the catalytic process. We can recall that the only three active catalysts are FTF4, DPB, and DPA, two group 2 compounds and one group 1 compound. However, a puzzling fact is that the ordering of the interactions in intensity for the nonelectroactive derivatives is exactly the same as in the case of the cobalt derivatives previously reported.[21a] This argument again leads back to the question regarding the assignment of the redox site in the case of the dicobalt derivatives. In a subsequent paper, the electrochemical properties and oxygen reactivity of the cobalt dimers[21c,d] will be reexamined more thoroughly in light of the present findings. The admixture of the redox processes centered on the cobalt with those on the rings will be clarified, and the implication of the π–π interactions in the reactivity toward O_2 will be scrutinized.

Acknowledgment. The CNRS (Unité Associée D0322), NSF, and NIH are gratefully acknowledged for support of this work.